Semiempirical molecular orbital calculations on benzene and 9-methylguanine
by David Theiste

A thesis submitted in partial fulfillment of the requirements for the degree of Doctor of Philosophy in Chemistry
Montana State University

Abstract:
Electrostatic perturbations of electronic states have been studied in light of two failures of semiempirical molecular orbital calculations. The polarization of the molecular orbitals caused by the electrostatic effects from the normal modes in benzene and the crystal environment in guanine plays a key role in understanding the roots of these failures.

The first failure, the failure of CNDO/S methods to accurately predict the relative oscillator strengths induced by the two e2g modes V6 and V8 in the lowest excited state in benzene, is found to lie in the formula typically used for the electron repulsion integrals, and not in the form of the normal modes used. A straightforward perturbation equation for the mixing of molecular states has been devised which involves the overlapping of the transition density matrix and the Fock perturbation matrix. This equation gives an accurate approximation for the mixing of the forbidden Lb state and the allowed Bb state in benzene. The inclusion of polarization of the molecular orbitals leading to electron density changes in the molecule is central to the understanding of vibronic coupling in this analysis.

The second failure, the failure of INDO/S calculations in estimating the transition dipole moment directions of the lowest two ππ states in 9-ethylguanine is found to lie in neglecting crystal field effects in the Hamiltonian used. By including the crystal electric field and electrostatic potentials, the calculated transition moments are found to agree with Clark's (1972) single crystal results. The same perturbation equation that predicts benzene vibronic coupling activity also accurately predicts the mixing of the excited states caused by the field in guanine. The results of this work indicate that the transition moment directions are sensitive to the environment and may be quite different in DNA itself than in the crystal.

Semiempirical molecular orbital calculations were also applied to the study of the vibronic and nonadiabatic coupling caused by the b2u normal mode V14 in benzene. The perturbation theory developed in this work predicts this mode to directly couple the 1B2u (Lb) state to the ground state in benzene. This coupling identifies V14 as a possible suspect in the search for a cause of the "Channel Three" phenomenon.

SEMIEMPIRICAL MOLECULAR ORBITAL CALCULATIONS ON BENZENE AND 9-METHYLGUANINE

by

David Theiste

A thesis submitted in partial fulfillment
of the requirements for the degree

of

Doctor of Philosophy

in

Chemistry

MONTANA STATE UNIVERSITY
Bozeman, Montana

October, 1989

APPROVAL

of a thesis submitted by

David Theiste

This thesis has been read by each member of the thesis committee and has been found to be satisfactory regarding content, English usage, format, citations, bibliographic style, and consistency, and is ready for submission to the College of Graduate Studies.

Oct 12, 1989
Date

Patrick R Callis
Chairperson, Graduate Committee

Approved for the Chemistry Department

Oct 12 1989
Date

Edwin H. Abbott
Head, Chemistry Department

Approved for the College of Graduate Studies

October 17, 1989
Date

Henry L Parsons
Graduate Dean

STATEMENT OF PERMISSION TO USE

In presenting this thesis in partial fulfillment of the requirements for a doctoral degree at Montana State University, I agree that the Library shall make it available to borrowers under rules of the Library. I further agree that copying of this thesis is allowable only for scholarly purposes, consistent with "fair use" as prescribed in the U.S. Copyright Law. Requests for extensive copying or reproduction of this thesis should be referred to University Microfilms International, 300 North Zeeb Road, Ann Arbor, Michigan 48106, to whom I have granted "the exclusive right to reproduce and distribute copies of the dissertation in and from microfilm and the right to reproduce and distribute by abstract in any format."

Signature David Theisen

Date Oct 12, 1989

This thesis is dedicated to the loving memory of Steffen Hans Theiste. Even though his time with the author was short, his life and death had a great impact on the lives of everyone around him.

ACKNOWLEDGMENTS

Without the love and support provided by Beth Ann, Eric and Anders Theiste the author could have never completed the research described in this thesis. Their patience and understanding over the years is gratefully acknowledged.

The help and effort of Professor Patrik Callis in lending his guidance and support is cheerfully acknowledged. The help and friendship of Dr. Richard D. Jones is also greatly appreciated.

Financial support from the Department of Chemistry at Montana State University and the National Institutes of Health made this work possible. Computer time from the M.S.U. Office of Systems and Computing Services is also greatly appreciated.

TABLE OF CONTENTS

LIST OF TABLES

LIST OF FIGURES

ABSTRACT

Electrostatic perturbations of electronic states have been studied in light of two failures of semiempirical molecular orbital calculations. The polarization of the molecular orbitals caused by the electrostatic effects from the normal modes in benzene and the crystal environment in guanine plays a key role in understanding the roots of these failures.

The first failure, the failure of CNDO/S methods to accurately predict the relative oscillator strengths induced by the two e_{2g} modes ν_6 and ν_8 in the lowest excited state in benzene, is found to lie in the formula typically used for the electron repulsion integrals, and not in the form of the normal modes used. A straightforward perturbation equation for the mixing of molecular states has been devised which involves the overlapping of the transition density matrix and the Fock perturbation matrix. This equation gives an accurate approximation for the mixing of the forbidden L_b state and the allowed B_b state in benzene. The inclusion of polarization of the molecular orbitals leading to electron density changes in the molecule is central to the understanding of vibronic coupling in this analysis.

The second failure, the failure of INDO/S calculations in estimating the transition dipole moment directions of the lowest two $\pi\pi^*$ states in 9-ethylguanine is found to lie in neglecting crystal field effects in the Hamiltonian used. By including the crystal electric field and electrostatic potentials, the calculated transition moments are found to agree with Clark's (1972) single crystal results. The same perturbation equation that predicts benzene vibronic coupling activity also accurately predicts the mixing of the excited states caused by the field in guanine. The results of this work indicate that the transition moment directions are sensitive to the environment and may be quite different in DNA itself than in the crystal.

Semiempirical molecular orbital calculations were also applied to the study of the vibronic and nonadiabatic coupling caused by the b_{2u} normal mode ν_{14} in benzene. The perturbation theory developed in this work predicts this mode to directly couple the $^1B_{2u}$ (L_b) state to the ground state in benzene. This coupling identifies ν_{14} as a possible suspect in the search for a cause of the "Channel Three" phenomenon.

INTRODUCTION

In the study of molecular properties, semiempirical molecular orbital methods have gained wide acceptance. For example, calculations of the ratio of the vibrationally induced transition intensity of the two lowest $\pi\pi^*$ states in benzene, L_b and L_a, are predicted within 10% accuracy. They do not perform perfectly, however. An example is found in calculations of the vibrationally induced intensity of the dipole forbidden L_b ($^1B_{2u}$) band in benzene. Absorption intensity in this band derives mainly from vibronic coupling to the dipole allowed $B_{a,b}$ ($^1E_{1u}$) states, with the e_{2g} mode, ν_6, contributing the bulk of the induced integrated absorption, or oscillator strength.[1] Semiempirical calculations, such as CNDO/S or INDO/S predict the ratio of the integrated absorption for the two modes, or f_6:f_8, to be approximately two to one.[2] Using excited state modes increases this ratio to four to one.[3] However, the experimentally observed ratio is much larger -- on the order of one hundred to one.[4,5]

Another area in which the semiempirical calculations have been questioned is in the study of the DNA bases. In one case, the calculated transition dipole moment directions for the two lowest $\pi\pi^*$ states of 9-ethylguanine, the calculated transition moment directions are at odds with experimental single crystal absorption measurements by about 50°.[6-8]

These failures, if they are caused by shortcomings in the theory, could lead to dismissing results from these types of calculations.

This work answers the question, "Are these discrepancies indicative of a general failure of semiempirical calculations, or are they the result of an

incomplete or inaccurate physical description of the system?" More specifically for benzene, "Are the normal mode displacements used in typical CNDO/S calculations accurate or not?" And in guanine, "Is an isolated molecule really like the molecule inside a crystal?"

These two problems are not at all unrelated. The perturbation caused by the distortion of the benzene molecule along a normal mode must change the environment at the atomic centers in order for the L_b state to couple to the B_b state and be seen in the absorption spectrum. This requirement of electronic changes at atomic centers plays an important role in the understanding of the vibronic coupling mechanism. In the case of guanine, the crystal environment could lead to changes in the potential seen by an atom. These potential changes then could lead to mixing of the electronic states. Thus, electrostatic effects and how they change the calculated spectra of these two molecules are at the heart of this work.

The third area that will be covered in this work is the vibronic coupling caused by the two-photon active b_{2u} mode (ν_{14}). There has been a debate as to whether or not this mode can couple the ground state directly to the lowest excited $\pi\pi^*$ state, L_b, in benzene.[9,10] Inspection of the pattern required to directly couple the ground and L_b states suggests that off-diagonal electronic changes are important, this is exactly the perturbation that ν_{14} would have on benzene. If this coupling actually occurs then, in a benzene system constrained to remain planar, ν_{14} would be a likely candidate for a promoting mode that can lead to a direct internal conversion process from the first excited state to the ground state.

Background

Studies of the lowest excited states of the cata-condensed hydrocarbons revealed similar patterns in many of these molecules. Observations of the ultraviolet region of the absorption spectra also contain some similarities. First, that the ultraviolet absorption region consisted of three bands and second, the relative intensity of the bands tends to increase with energy.[11] The benzene system serves as a prototype for the study of the absorption spectrum of the cata-condensed hydrocarbons because of its high symmetry, D_{6h}. Theoretical descriptions of the benzene excited states based on the π molecular orbitals gave reasonable qualitative agreement with experimental results for benzene, but became complex for larger systems.[12,13] Worse yet, these calculations did not give quantitative agreement with the energies of observed bands. A general theory was required to understand the excited states in general and the lowest excited state in particular[14] of aromatic molecules in order for further developments to be made.

Platt[15] devised a method whereby he classified the electronic states of an aromatic hydrocarbon based on a particle constrained to a ring of radius r. The solutions to the quantum mechanical particle in a one-dimensional loop problem are functions of the form $e^{im\varphi}$ where m is the angular momentum of the particle. Platt used, as Hückel[16] had done, the concept of "mobile"[17] electrons, electrons free to move around the ring. Platt also followed Hückel's use in benzene of the "orbital ring quantum number," m, to describe the angular momentum of the electron and their addition and subtraction to give the "total ring quantum

number." This model gives rise to 3 bands in the cyclic aromatic hydrocarbons. Platt labeled them based on changes in total ring quantum number when the molecule absorbed light. The weak, lowest energy band is called L_b, the second band L_a, and the most intense band, B_a and B_b. In monocyclic aromatic hydrocarbons like benzene, the two B states are degenerate. In cata-condensed hydrocarbons with n rings and a general formula $C_{4n+2}H_{2n+4}$, the values of m run in the range of $-(2n+1) \leq m \leq (2n+1)$, with an electron having an energy that depends on the absolute value of m. Thus, orbitals with opposite signs for m have the same energy.

The pairing, or finding of orbitals that have identical energies, of the molecular orbitals is shown in Figure 1 where the orbitals of benzene are depicted in the atomic orbital representation, where the size of the circle is proportional to the coefficient of the respective p_z atomic orbital at that center. In Figure 2 these same orbitals of benzene are plotted in 3-dimensional position space. The contours represent an absolute value of the wavefunction greater than .05. These orbitals, are not the same as the orbitals Platt used, that is, they are not eigenfunctions of the angular momentum operator. However, they show the same patterns of nodes perpendicular to the molecular plane as the states in angular momentum space would. The degenerate eigenfunctions, $\pm|1^A\rangle$, of the angular momentum operator can be constructed from the orbitals shown in Figure 1. The linear combinations $|2\rangle \pm i|3\rangle$ give $\pm|1^A\rangle$. This is similar to the atomic orbitals p_x and p_y. They form the eigenfunctions of the angular momentum operator L_z by $p_x \pm ip_y = p_{\pm 1}$.

Several points should be noted about the orbitals pictured in Figures 1 and 2; first, the pairing of orbitals 2 and 3. They are degenerate, as are the orbitals labeled 2′ and 3′. Next, there is also a pairing between an occupied orbital and

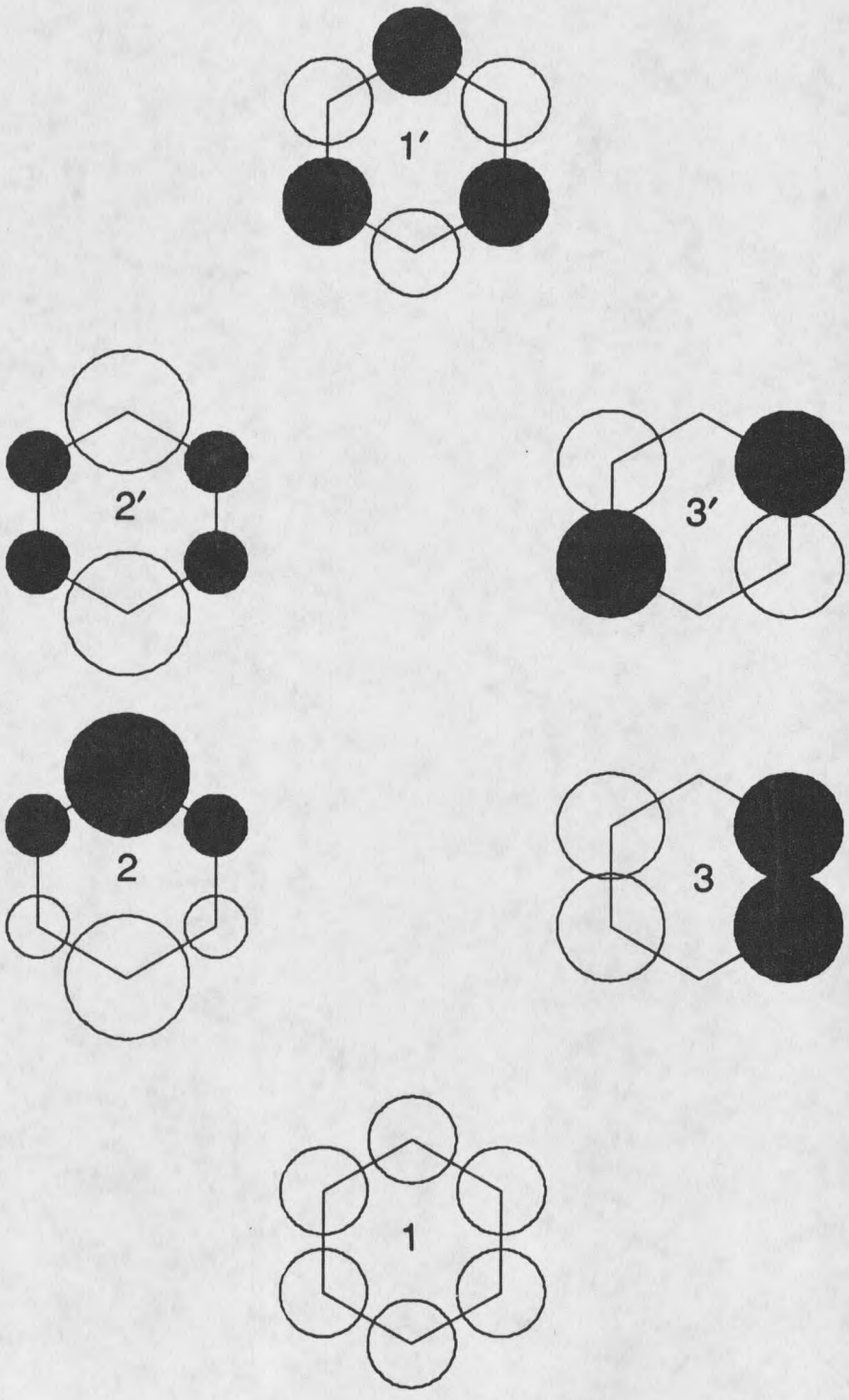

Figure 1. The six π molecular orbitals of benzene in the atomic orbital representation.

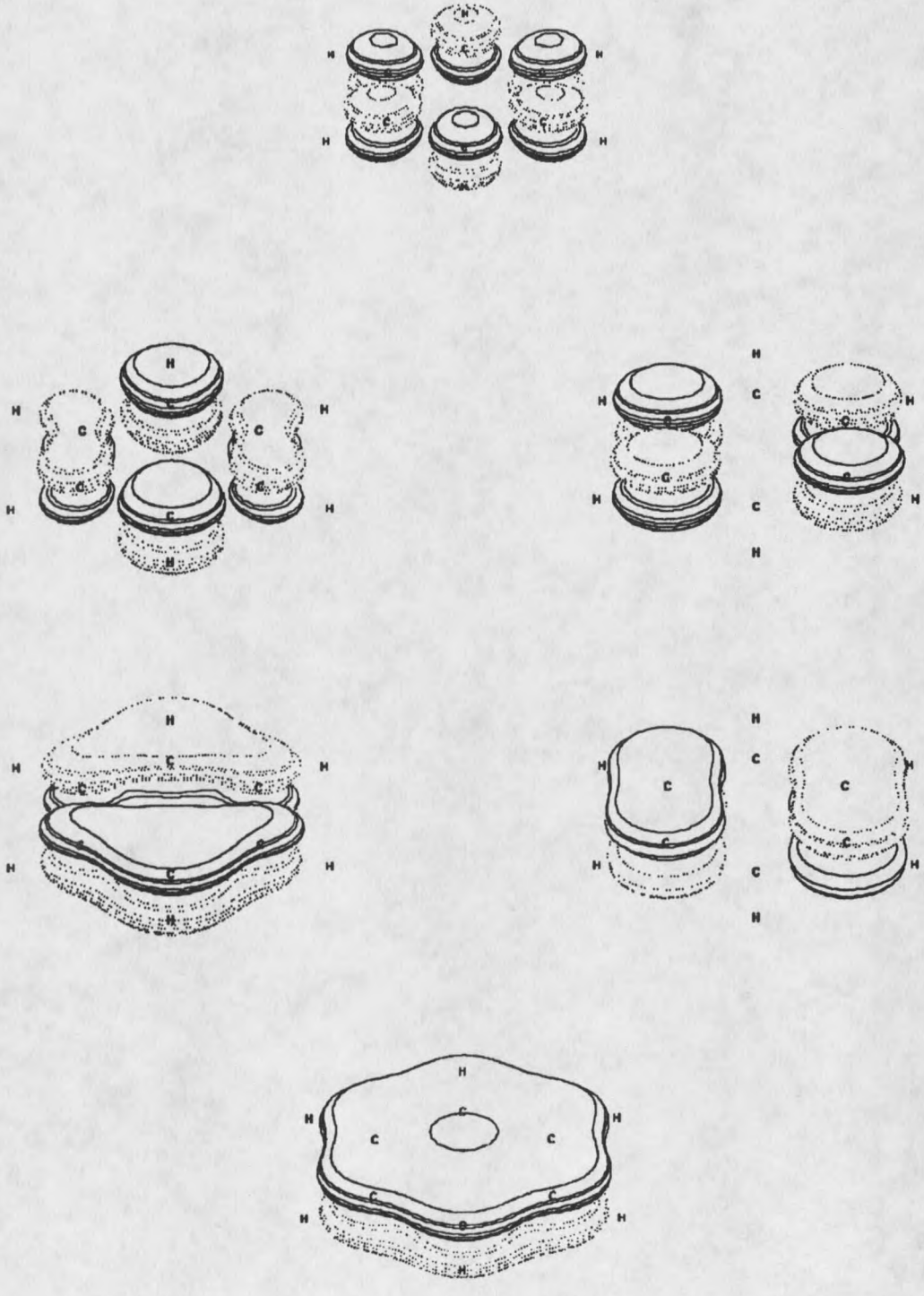

Figure 2. The six π molecular orbitals of benzene.

a virtual, or unoccupied orbital, for example 3 and 3′. The magnitudes for each atomic orbital coefficient are the same for each of the so called pseudo-, or image paired orbitals with the sign of the coefficient on every other atomic center changed.

Moffitt[18] later applied to Platt's perimeter model a linear combination of atomic orbitals for the carbon atoms on the ring. He then applied perturbation theory to the unperturbed states to construct higher homologs of benzene.

One of the most revealing results of Moffitt's work was the division of the perturbation matrix into an "even" and an "odd" matrix. An "even" perturbation is one that affects "even" positions in the matrix, that is positions whose indicies sum to an even number. Similarly, "odd" perturbations affect odd positions in the matrix. For example, the matrix

$$\begin{pmatrix} a & b \\ c & d \end{pmatrix}$$

can be written as the sum of an "even" matrix,

$$\begin{pmatrix} a & 0 \\ 0 & d \end{pmatrix}$$

and an "odd" matrix,

$$\begin{pmatrix} 0 & b \\ c & 0 \end{pmatrix}$$

regardless of the values of a, b, c and d. Under this division inductive perturbations, such as exchanging an H for a F or a C for an N in benzene, are considered to be "even." Stretching vibrations, on the other hand, are mainly "odd." Moffitt also demonstrated that the L_b and L_a states of benzene also had "even" or "odd" character. He did this by calculating the effect of an "even" or "odd" perturbation on the states and found, in agreement with experiment, that "even" perturbations enhanced the L_b state more than the L_a and that "odd"

perturbations had the opposite effect. McLachlan[19] and Donath[20] later explained this "even" or "odd" property of the states of an alternate hydrocarbon in terms of electron configurations. McLachlan noted that radical cations were related to radical anions by "image pairing" of electrons and holes. He also noted that a neutral molecule contained its own "image pair" and that every state was either even or odd based on the effect a "pairing operation" had on the state. Thus, a configuration which was symmetrically excited, that is an electron is taken from orbital i and placed in i′, its own pair, is even. All other configurations give both the even and odd combinations. The state is even if the configurations are added and if they are subtracted the state is odd. Pariser[21] showed that these even and odd characters gave rise to the dipole selection rules with (even ↔ odd) transition being allowed and (even ↔ even) being forbidden. This even or odd property is now known as pseudoparity.[22]

To help visualize the concept of a configuration, Figure 3 is included. This figure shows a molecular orbital diagram with the dashed arrows representing the excited configurations for both the L_a and L_b state. In the case of the L_b state, for example, the two crossed arrows each represent an excited configuration; one arrow represents removing an electron from the orbital 2 and placing it into orbital 3′, the other arrow represents transferring an electron from orbital 3 to orbital 2′.

Callis, Scott and Albrecht[22] later generalized the pseudoparity perturbation selection rules for various types of spectroscopy. To determine if two states $\Psi(i)$ and $\Psi(j)$ will be mixed under the influence of a perturbation $\mathbb{H}'$ the matrix element $\langle\Psi(i)|\mathbb{H}'|\Psi(j)\rangle$, must be calculated. McWeeny[23] showed that

$$\langle\Psi(i)|\mathbb{H}'|\Psi(j)\rangle = \mathrm{tr}(\mathbb{H}'\rho^{ij}) = \sum_{r,s} H'_{rs}\rho^{ij}_{sr},$$

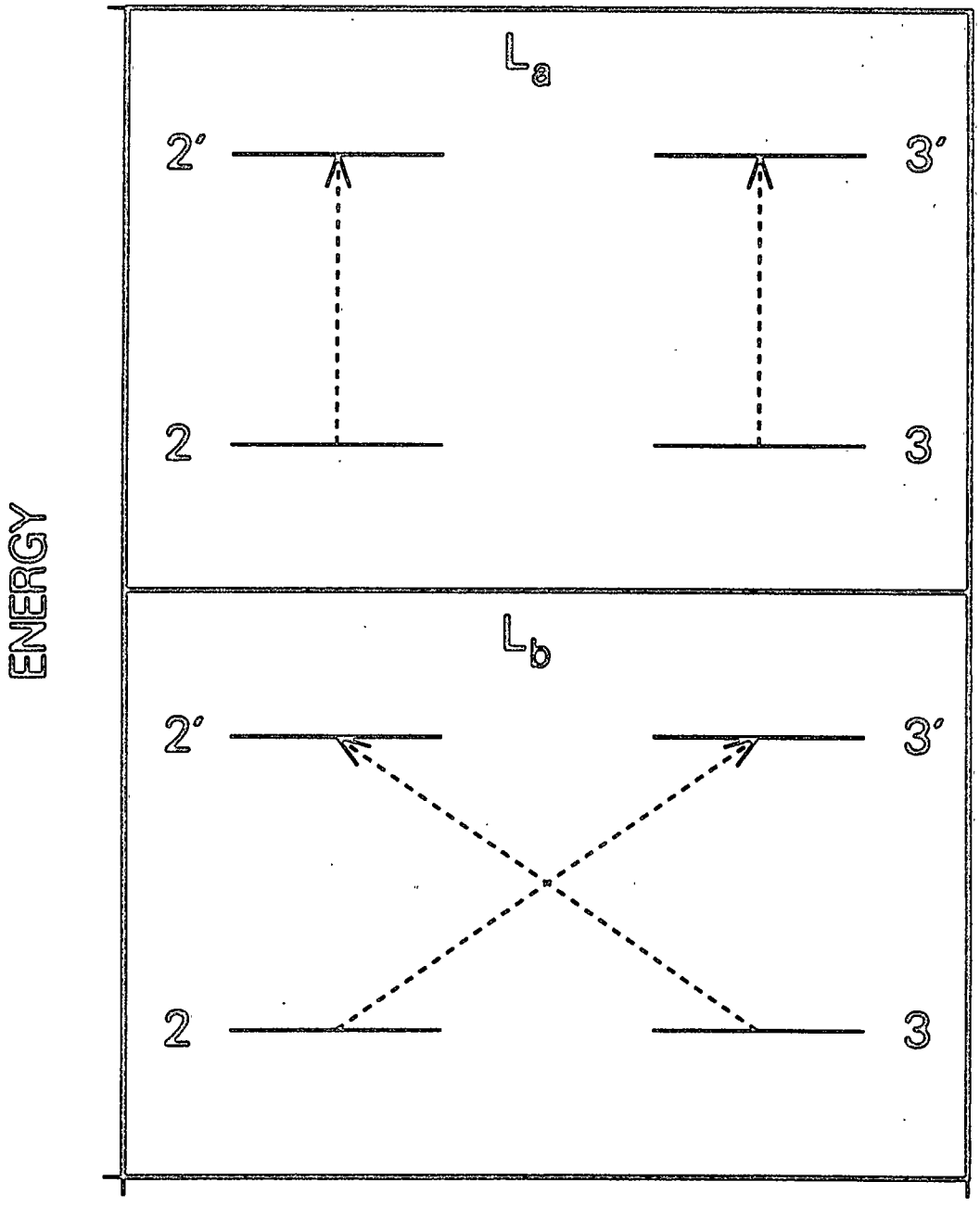

Figure 3. Pictorial view of the L_b and L_a states in benzene

where ρ^{ij} is $|\Psi(i)\rangle\langle\Psi(j)|$ and is the first order reduced transition density operator. Here, $\mathbb{H}'$ is a one-electron operator. The tr in the equation means trace, the sum of the diagonal matrix elements of the product. Callis, Scott and Albrecht also noted that the separation of the transition density operator into a symmetric and antisymmetric part, or bond order and antibonding order matrices, projects out the real and imaginary parts of the perturbation matrix $\mathbb{H}'$. They then showed that the transition bond order matrices between states have even or odd character, just as the states do. Transition bond orders between states of the same pseudoparity are odd and transition bond orders between states of opposite, or different pseudoparity are even. This property of the transition bond orders was then shown, as Donath had done, to have the effect that inductive perturbations, being even, coupled states of opposite pseudoparity. Similarly, stretching vibrations, being odd, would couple states with the same pseudoparity.

In benzene the L_b state being a minus state can only be coupled to the allowed B states by an even perturbation, conversely the L_a being plus is coupled to the allowed states by an odd perturbation. Vibrational stretching modes (odd perturbations) then result in the absorption of the L_a band being moderately intense, while these motions have little effect on the L_b band, and it is observed to be weak.

The transition bond orders between both the L_b and L_a states of benzene and the ground state are shown in Figure 4 in the space of the square of the atomic orbitals. That is, a diagonal position gives the amount of the p_z atomic orbital squared at that center and off-diagonal positions are the product of the two p_z orbitals on the adjacent positions. The black or filled circles are minus in sign and open or white circles are positive. These same transition bond orders are shown in Figure 5 in position space. These two figures demonstrate

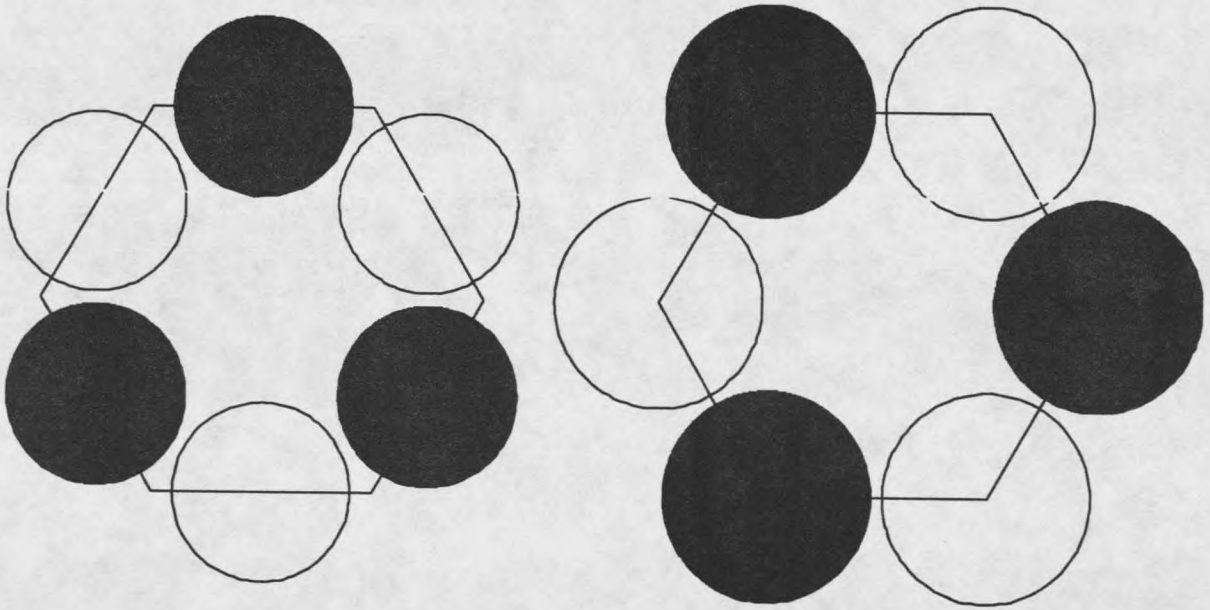

Figure 4. The transition bond orders for the L_b and L_a state in benzene.

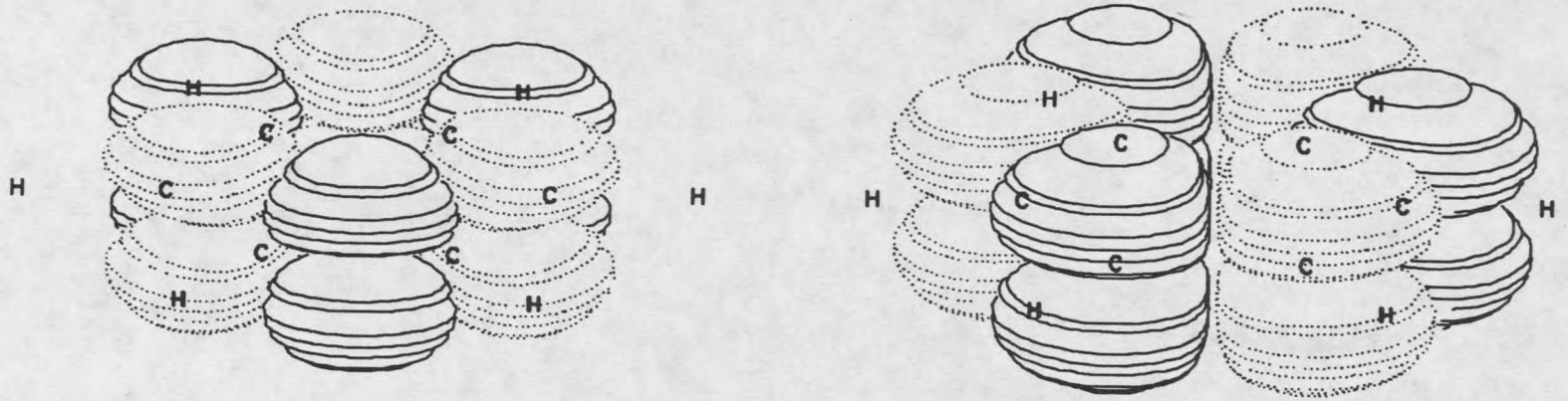

Figure 5. The transition densities for the L_b state (left) and the L_a state (right) in benzene.

the difference between transition bond orders between states of the same pseudoparity and states of opposite pseudoparity. The ground state being minus only has nonzero off-diagonal (odd) matrix elements in the transition bond order to the L_b state and has nonzero diagonal matrix elements (even) in the transition bond order to the L_a state.

The quantity $tr(H'\rho^{ij})$ can be rewritten in a more convenient form in which the overlap of the matrices H' and ρ^{ij} is more easily determined. The operation "double dot product," written $H':\rho^{ij}$ is simply the multiplication of corresponding elements in the two matrices and then summing over the entire resulting matrix. This direct mapping is useful in visualizing the effect a perturbation must have in order to effectively couple two states. The two matrices must have the same form in order to have a large overlap.

Concurrent with these developments, other workers were working out the problem of expressing the nuclear portion of the states. Shortly after the introduction of quantum mechanics, Born and Oppenheimer[24] justified and derived an expression for the separation of the total molecular wavefunction into an electronic part and a vibrational, or nuclear part. This method of solving this problem is rooted in the fact that a proton has 2000 times the mass of an electron. Compare for instance the mobility of a hiker carrying a pint of water and another hiker burdened with a bottle of water three and a half feet across and three feet tall. That is the electron to nuclear mass ratio for a hydrogen atom. Our hiker would need twelve such bottles for the relative mass of a carbon nucleus. Starting with the time independent Schrödinger equation,

$$H(q,Q)|\Psi_i(q,Q)\rangle = \varepsilon_i|\Psi_i(q,Q)\rangle,$$

where $|\Psi_i(q,Q)\rangle$ is the i^{th} wavefunction for the molecule, q represents the coordinates for the electrons, Q the coordinates for the nuclei, and ε_i is the i^{th}

eigenvalue or energy. H(q,Q) is the total molecular Hamiltonian written as

$$H(q,Q) = T_e(q) + T_N(Q) + U(q,Q),$$

where $T_e(q)$ is,

$$T_e(q) = -\sum_i \frac{p_i^2}{2m},$$

and $T_N(Q)$ is

$$T_N(Q) = -\sum_k \frac{P_k^2}{2M_k}.$$

These terms are then added to the potential energy of the electron-nuclear attractions and electron-electron and nuclear-nuclear repulsions, U(q,Q). The exact solutions to this equation cannot be obtained since the Hamiltonian does not allow for the separation of the variables, q and Q. Born and Huang[25] (BH) approached the problem by separating the total Hamiltonian into two parts. The first part involves only the electronic energy and is written,

$$H_e(q,Q) = T_e(q) + U(q,Q).$$

This is known commonly as the electronic Hamiltonian. Eigenfunctions of this Hamiltonian are the electronic wavefunctions and they satisfy the time independent Scrödinger equation

$$H_e(q,Q)|\psi_n(q,Q)\rangle = E_n(Q)|\psi_n(q,Q)\rangle,$$

where $E_n(q,Q)$ is the energy of the n^{th} electronic eigenstate or eigenfunction and depends on Q as a parameter. The total wavefunction is then written as a linear combination of the electronic wavefunctions

$$|\Psi_i(q,Q)\rangle = \sum_n |\psi_n(q,Q)\rangle|\chi_{ni}(Q)\rangle,$$

where the χ_{ni} are the expansion coefficients and they depend explicitly on Q. The total molecular Hamiltonian is then applied on this wavefunction

$$[H_e + T_N(Q)]\sum_n ||\psi_n(q,Q)\rangle|\chi_{ni}(Q)\rangle = \varepsilon_i \sum_n |\psi_n(q,Q)\rangle|\chi_n(Q)\rangle.$$

Using the definition of $T_N(Q)$ on the linear combination wavefunction gives

$$T(Q)|\psi_n(q,Q)\rangle|\chi_{ni}(Q)\rangle = \sum_k [T(Q)|\psi_n(q,Q)\rangle]|\chi_{ni}(Q)\rangle + |\psi_n(q,Q)\rangle[T(Q)|\chi_{ni}(Q)\rangle]$$

$$- \frac{1}{2M_k} P_k|\psi_n(q,Q)\rangle P_k|\chi_{ni}(Q)\rangle.$$

Recalling that

$$P_k = -i\hbar \frac{d}{dQ_k} = -i\hbar \nabla_k,$$

leads to

$$\sum_k \sum_n \Big(\{ |\psi_n(q,Q)\rangle [T(Q) + E_n(Q)] + [T(Q)|\psi_n(q,Q)\rangle] \} |\chi_{ni}(Q)\rangle$$

$$- \frac{\hbar^2}{M_k} [\nabla_k|\psi_n(q,Q)\rangle \times \nabla_k|\chi_{ni}(Q)\rangle] \Big) = \varepsilon_i \sum_n |\psi_n(q,Q)\rangle|\chi_{ni}(Q)\rangle.$$

Then this equation is multiplied by $\langle\psi_n(q,Q)|$. Remembering that the electronic wavefunctions are orthonormal, gives rise to

$$[T(Q) + E_n(Q) + \langle\psi_n(q,Q)|T(Q)|\psi_n(q,Q)\rangle - \varepsilon_i]|\chi_{ni}(Q)\rangle$$

$$+ \sum_k \sum_{n \neq m} \Big[\langle\psi_n(q,Q)|T(Q)|\psi_m(q,Q)\rangle - \frac{\hbar^2}{M_k} \langle\psi_n(q,Q)|\nabla_k|\psi_m(q,Q)\rangle \nabla_k \Big] \chi_{mi} = 0.$$

The approximation BH makes now is known as the BH adiabatic approximation[26] and consists of elimination of the off diagonal electronic matrix elements; that is the last two terms in the equation are taken to be zero. Consider again the two hikers. The hiker saddled with the large bottle of water only affects the hiker with the pint bottle by where he is. The hiker who can move rapidly can consider his fellow outdoorsman to be confined to one spot as he moves around the countryside. In this approximation the total wavefunction, $\Psi_{ni}(q,Q)$, is

$$\Psi^A_{ni}(q,Q) = \psi_n(q,Q)\chi^A_{ni}(Q).$$

The index n means the wavefunction associated with the electronic state n and superscript A means adiabatic. The χ_{ni} were the expansion coefficients originally. However, in this case they have additional meaning, they are also the eigenfunctions of the time independent Schrödinger equation

$$[T(Q) + E_n(Q) + \langle\psi_n(q,Q)|T(Q)|\psi_n(q,Q)\rangle - \varepsilon_{ni}]\chi_{ni}(Q) = 0.$$

This is the equation whose solution is the vibrational wavefunction.[26]

Two additional approximations are:

1) The Born-Oppenhiemer adiabatic approximation, where the term

$$\langle\psi_n(q,Q)|T(Q)|\psi_n(q,Q)\rangle$$

is taken to be zero, and the total approximate wavefunction is

$$\Psi^{BO}_{n\,i}(q,Q) = \psi_n(q,Q)\chi^{BO}_{n\,i}(Q),$$

and the solution for the vibrational wavefunction is

$$[T(Q) + E_n(Q) - \varepsilon_{ni}]\chi^{BO}_{n\,i}(Q) = 0.$$

2) The crude adiabatic approximation where the electronic wavefunctions are calculated at a fixed nuclear geometry. The geometry generally chosen is the equilibrium geometry. Here the total approximate wavefunction is

$$\Psi^{C}_{ni}(q,Q) = \psi_n(q,Q_0)\chi^{C}_{ni}(Q),$$

and the equation yielding the vibrational wavefunction is

$$[T(Q) + E_n(Q_0) + \langle\psi_n(q,Q)|\Delta U(q,Q)|\psi_n(q,Q)\rangle - \varepsilon_{ni}]\chi^{C}_{ni}(Q) = 0.$$

Herzberg and Teller,[27] (HT) in considering the vibrational structure of an electronic transition band, demonstrated that a state Ψ_i of a molecule at a geometry distorted from equilibrium can be written, to first order, as a sum over all the states of the molecule at the equilibrium geometry, or

$$\Psi_i(q,Q) = \sum_j c_{ij}(Q)\Psi_j(0),$$

where c_{ij} is the amount of state $\Psi_j(0)$ that is "mixed into" the state $\Psi_i(Q)$. The coefficient c_{ij} can be written as

$$c_{ij}(Q) = \frac{H'_{ij}(Q)}{E^\circ_i - E^\circ_j},$$

where H'_{ij} is the mixing of the states caused by the perturbation, in this case, the motion of the nuclei. The denominator is the energy separation between the two

states. This expression for c_{ij} applies only when $i \neq j$. "What is the nature of H'_{ij}?" To first order it is commonly written as

$$H'_{ij} = \left(\frac{\partial H_e}{\partial Q_k} \right)_{Q_0} Q_k,$$

for a molecular vibration k, with the only Q dependence in H_e being the attraction between the nuclei and the electrons, or V_e. V_e is written as

$$V_e = \sum_{i}^{I} \sum_{n}^{N} Z_n \frac{e^2}{r_{in}},$$

where Z_n is the nuclear charge minus the number of core electrons for atom n, and r_{in} is the distance between electron i and nucleus n. Assuming the coupling to be linear in the displacement along the normal mode Q_k, the coupling between two Born Oppenheimer (BO) states is

$$\langle \psi_n(q,Q) | (\nabla_k H) | \psi_m(q,Q) \rangle \langle \chi_{ni}(Q) | Q_k | \chi_{mj}(Q) \rangle,$$

leading to the well known selection rule that

$$j = i \pm 1.$$

Traditionally, the quantity Z_n has been taken to be constant, that is the core electrons are assumed to perfectly follow the nuclei as they move. This approximation of constant electron density on the atomic centers leaves only changes in distance, the r_{in}^{-1} term in the derivative with respect to Q.

An additional approximation has been made to the normal HT expansion in which the atomic orbitals float along with the nuclei as they move.[28] This approximation greatly reduces the number of orbitals required to include the major effects of the shifting of the nuclear positions.

This HT expansion has only been applied to the final or excited state in this discussion. A similar treatment can be carried out for the ground state, as has been done by Ziegler and Albrecht.[2] Using CNDO they calculated the

correction to the transition moment of the L_b state in benzene by including ground state coupling to the excited states. They found the correction to the TM due to ground state coupling was small. Also, Ziegler and Albrecht calculated the BO breakdown coupling in the L_b state and concluded that the correction to the HT coupling was small (about .02 times the HT coupling). So, in calculating vibronically induced intensity, the first order HT approach is quite realistic and typical HT calculations are done without including ground state mixing.

These formal approaches using only the π atomic orbital as a basis gave way to direct calculation of excited state properties by semiempirical molecular orbital calculations, first through the Pariser-Parr-Pople CI method[29] which was also restricted to a basis of the π molecular orbitals set and later to the all valence methods, such as CNDO/S.[30]

CNDO, which was developed in the mid-1960's by Pople and coworkers[31,32] along with INDO,[33] was reparameterized by Del Bene and Jaffé[34] in an effort to reproduce many observed features of the benzene spectra along with its analogs. Zerner[35] later did the same with INDO.

These semiempirical methods diagonalize the Hamiltonian matrix to give molecular orbitals as a linear combination of the atomic orbitals. From the atomic orbitals the Fock Hamiltonian matrix is constructed and molecular orbitals generated in the usual way. The states are constructed from configurations which are spin adapted Slater determinates. The configurations shown in Figure 3, for example, are expressed as a linear combination of an α spin electron being promoted and the promotion of a β spin electron. In this work, only the singlet states have been studied, however, calculations in triplet states can be performed. Singlet configurations are built simply by removing an electron from an occupied molecular orbital i and placing it in an unoccupied, or virtual molecular orbital j

and antisymmetrizing the state. They are written as χ_i^j. The energies of the configurations, $E(\chi)$, are then placed into a matrix along with interactions between the configurations. Then this so called configuration interaction matrix is diagonalized, with the resulting eigenvalues being the excited state energies and the eigenvectors being the excited states expressed as a linear combination of the individual excited configurations.

These calculational methods are currently the most straightforward and fastest way to calculate excited state properties such as oscillator strength, the one-photon absorption intensity integrated over an electronic state. They can also be used to calculate the direction of the transition dipole moment between the ground and excited state. These results can then be compared to experimental results from single crystal polarized absorption and reflection measurements.

In the case of the molecule 9-ethylguanine, shown in Figure 6, the results calculated by INDO/S are at odds with the observed transition moment directions. This disparity is listed in Table 1 and displayed in Figure 7 where the calculated transition moment directions are shown in the panel labeled "Theory (No Field)," along with the experimental results from Clark[8] in the panel labeled "Experiment." It can be seen that the predicted transition moments for the two lowest $\pi\pi^*$ transitions are rotated roughly 50° clockwise from the experimental values. The values for the lowest 5 $\pi\pi^*$ states are listed in Table 1. Callis[7] reported that changes in variables such as geometry, electron repulsion schemes and neglect of overlap, that is, using the CNDO or the INDO method, made only minor changes to the calculated transition moments. This apparent failure of INDO/S has left the validity of semiempirical methods in doubt when applied to the DNA bases.[6,7]

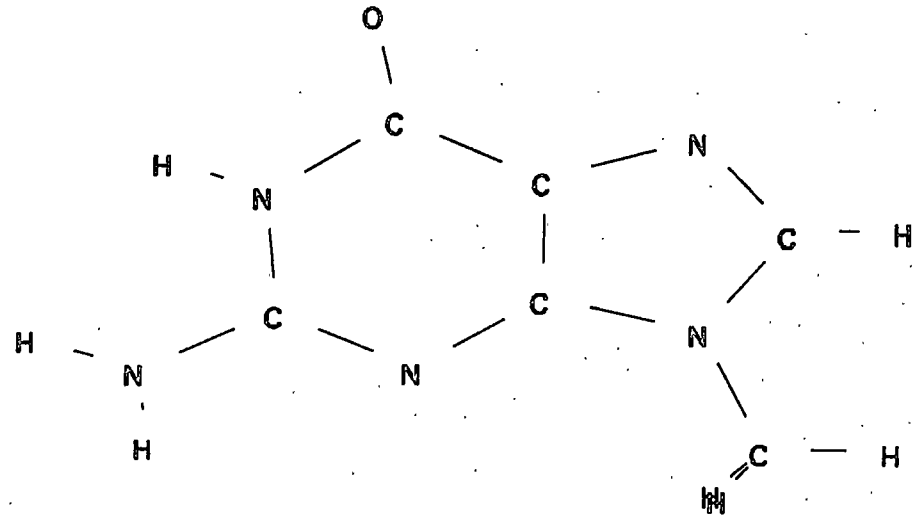

Figure 6. 9-ethylguanine.

Table 1. Comparison of experimental and calculated transition moment directions in 9-ethylguanine.

Calculated (No Field)			Experimental[a]		
λ(nm)	f[b]	θ(deg)[c]	λ(nm)	f	θ(deg)
314	0.294	-44	278	0.16	-4
274	0.383	57	254	0.25	105
241	0.012	-44	222	0.02	—[d]
209	0.501	56	204	0.41	-75
200	0.188	-61	189	0.48	(-9,41)e

[a] Ref 8
[b] Oscillator strength
[c] Convention of DeVoe and Tinoco,[36] measured clockwise from C_4-C_5 bond
[d] Direction not determined because of the low oscillator strength
[e] Subject to ambiguity. Clark preferred -9° based on a comparison with transition moment directions in guanine hydrochloride dihydrate, however, this argument is not conclusive.

Guanine, however, has a large ground state dipole moment[37] which changes significantly upon excitation.[38] The ground state dipole moment is shown in Figure 8 where the value for the total dipole moment is 9.05 Debyes and the

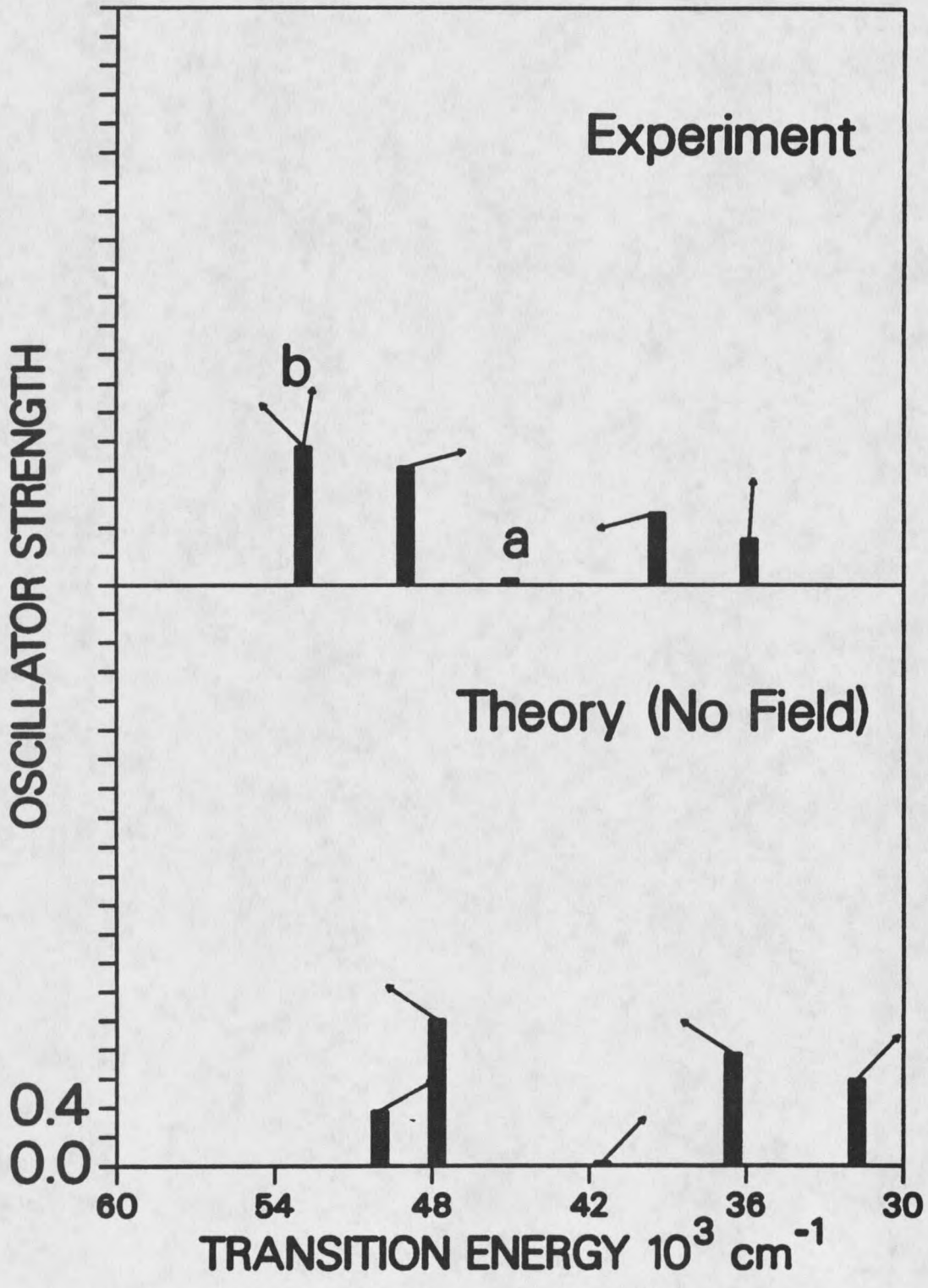

Figure 7. Comparison of theory and experimental results for 9-ethylguanine.

head of the arrow represents the positively charged end of the dipole moment vector. Neighboring molecules in the crystal then could, in principle, lead to alteration of excited state energies or large interactions between states. Woody[38] previously treated the molecular orbital predictions for the excited states of 9–ethylguanine calculated for the isolated molecule as a set of basis states and calculated the transition moments for the molecule in a crystal using the electrostatic interactions as a perturbation to the system. He found that the discrepancy was reduced by a factor of about two for the first two $\pi\pi^*$ states of 9-ethylguanine.

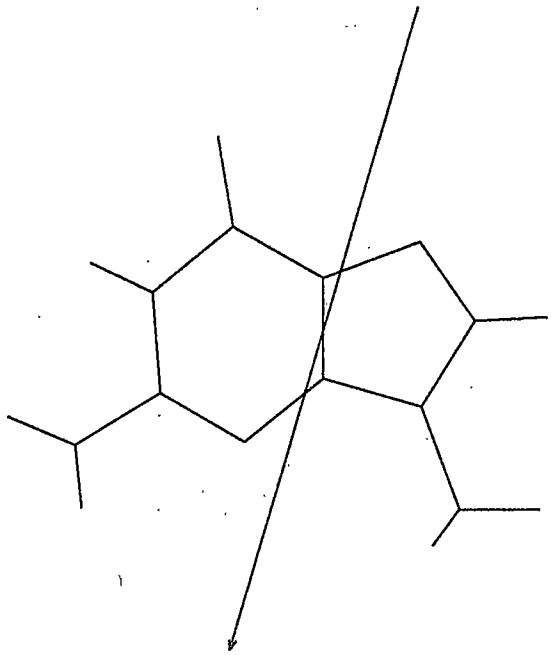

Figure 8. The ground state dipole moment of isolated 9-methylguanine calculated by INDO/S.

Statement of Problem

This work will address the failures referenced above. In the problem of calculating the relative vibronically induced oscillator strengths due to the normal modes ν_6 and ν_8 in benzene, CNDO/S and INDO/S calculations are used to discover if extensions to the area of vibronic coupling can be made. Specifically, it was a goal of this work to develop further understanding of the mechanism by which vibrations of the molecule affect its ability to interact with light. It also was a goal of this research to contribute to the ongoing discussion of the behavior of molecules while they are in the excited state.

This work also reports on the calculations of the transition moment directions by INDO/S methods and has as its goal determining if indeed semiempirical calculations are a viable tool in helping to explain the transitions observed in the DNA bases. The calculations undertaken for this thesis on 9–ethylguanine show that these methods can accurately predict the observed transition moments in the guanine chromaphore.

CALCULATIONAL METHODS

All calculations presented here were performed on the VAX 780 located in the Montana State University Computing Center until November, 1987 when the system was upgraded to a cluster of four VAX 8550s.

Calculations of transition dipole moments and one-photon oscillator strengths were done using INDO/S,[35] a semiempirical molecular orbital program developed by M. Zerner and coworkers over the past 20 years, kindly supplied to us by Dr. Zerner. Zerner's version of the program is quite useful for carrying out spectroscopic studies since a variety of options are available to the user such as CNDO/S and INDO/S along with several electron repulsion schemes and the ability to input various overlap variables. All of these options are available through the input data. The output from the INDO/S program was summarized using software developed by Professor Patrik Callis, which was also used to calculate two-photon intensities. In addition, the output was written out in a format suitable for use in plotting transition densities, that is, product functions of electronic states.

The INDO/S program was modified to include additional forms for electron repulsion integrals between two centers. Since the use of Coulomb's law in semiempirical methods, such as CNDO and INDO, does not accurately reflect the excited state energies, schemes have been developed which allow the calculated energies of the excited states in certain model compounds, for example benzene, to match the experimental transition energies. The most commonly used electron repulsion scheme in CNDO/S and INDO/S calculations was developed by Mataga

and Nishimoto (MN). Another scheme developed by Ohno and Klopman (OK) is more commonly used when doubly excited configurations are included in the calculations. These two electron repulsion schemes were included in the version of the INDO program used in these studies. The functional form for the electron repulsion of two carbon atoms for MN and OK, along with the theoretical R^{-1} value is shown in Figure 9. Others have modified these schemes, for example, the CNDO/S parameterization by Hug and Tinoco.[6] The modifications used in this work were made by adding four new variables to be read in and adding new program functions for calculating the electron repulsion between two centers, similar to the existing function named coul.

The INDO/S program was also modified during the course of this work to allow for inclusion of electric fields and electrostatic potentials for each atomic center in the input geometry. This modification gives the program the ability to include the effect of the electric field operator,

$$\vec{E} = -e\sum_{\alpha} \frac{q_\alpha}{R_{i\alpha}^3} \times \vec{R}_{i\alpha}.$$

The field is caused by the presence of charged particles outside the molecular frame. The field and the potential operator,

$$P_i = \sum_{\alpha} \frac{-eq_\alpha}{R_{i\alpha}},$$

were directly added to the Fock operator. This was accomplished by including a subroutine named elfld which added the potential to the F_{ii} term, the diagonal Fock matrix element. This subroutine also mixed the s atomic orbital with the p_α atomic orbital on the same atom because of the electric field oriented along the α direction, where α = X,Y,Z. For example, a s atomic orbital on a given

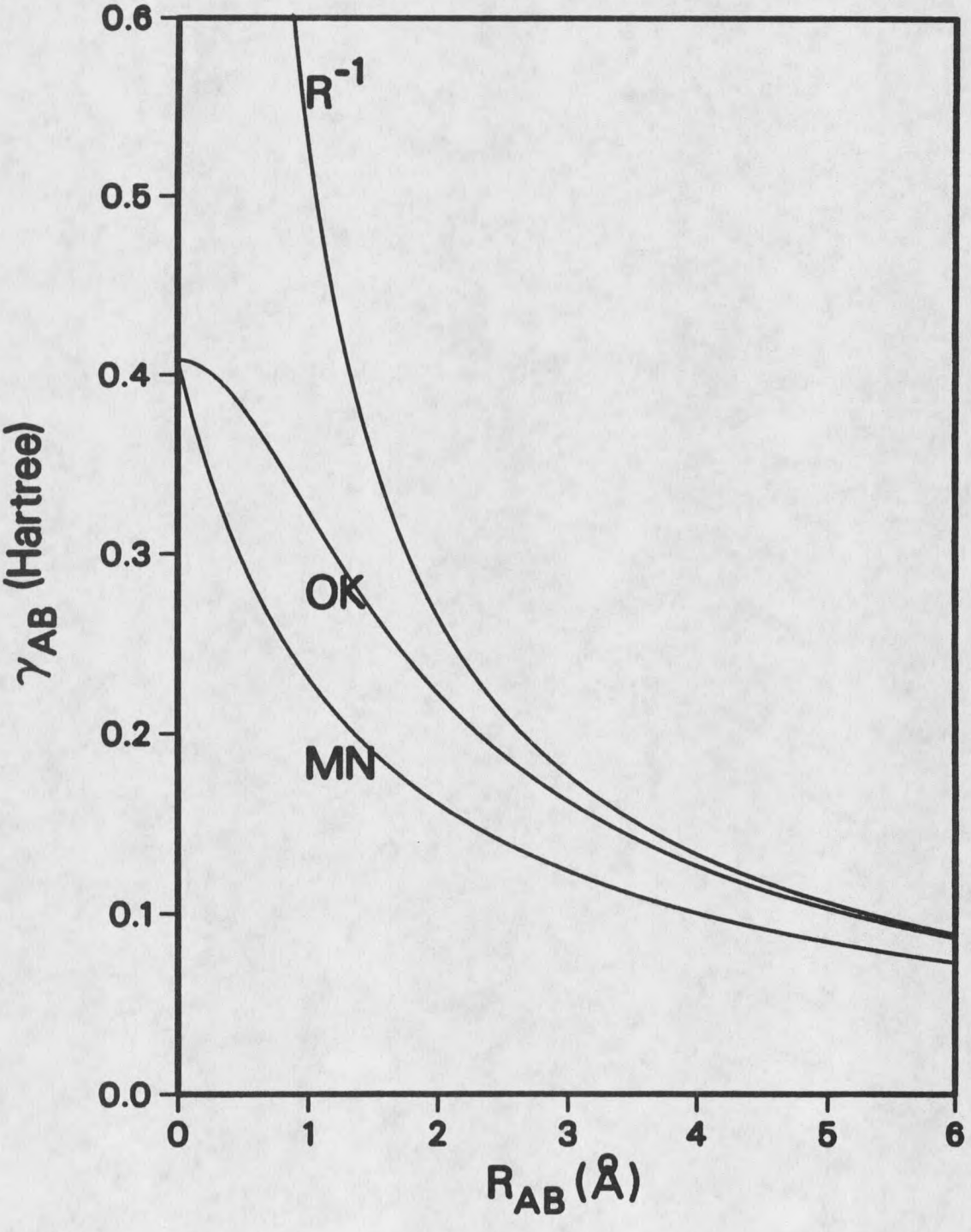

Figure 9. Typical electron repulsion schemes used in CNDO and INDO calculations.

carbon can mix with the p_z atomic orbital if the field at that atom has a component along the z axis.

Vibronic coupling calculations were carried out by moving the atomic coordinates one root-mean-square displacement from their equilibrium position in the INDO/S input file. The root-mean-square displacement is used because the induced oscillator strength can be directly calculated through the transition moment at this displacement.[39] The equilibrium geometry and normal modes used for the study of the benzene e_{2g} vibronic coupling activity were provided by L. Goodman and coworkers at Rutgers University. Additional calculations were also performed at various fractions of a root-mean-square displacement and using the negative phase of the displacement, that is distorting the molecule in the opposite direction of the coordinates supplied. This was done to check the linearity of vibronic coupling matrix elements. In all cases, deviations from linearity were negligible. In addition, linear combinations of modes were used in a portion of this study.

In the study of the transition moment directions of 9-ethylguanine, the molecule 9-methylguanine was used as the model compound, since differences due to the methyl and the ethyl substitution at the 9 position were deemed to be negligible. Since only minor changes in the calculated spectra were observed in going from guanine to 9-methylguanine, an iterative approach was taken for the 9-methylguanine calculations where the ground state dipole and nuclear charges were calculated and then sent to Professor Robert Woody at Colorado State University who then calculated the potential and electric field from the values of the atomic charges. The potential and field obtained were then added directly to the Fock operator in another INDO/S calculation which gave new values for the ground state dipole moment and atomic charges. This process was repeated until

convergence was obtained. The associated atomic charges were calculated in two ways. First, the diagonal elements of the density, or bond order, matrix were summed for all the basis orbitals assigned to a given atomic center to give an electron density P_A. The total charge on a given atom A is then given by $(Z_A - P_A)$. This manner of calculating the electron density is known as "being in the Löwdin basis." The second method to calculate the electron density is known as the Slater method or basis and it uses not the basis atomic orbitals in the density matrix, but a linear combination of these orbitals to give a set of orbitals centered around each atomic center. A second set of calculations was carried out using the fields scaled so that the ground state dipole moment as calculated by INDO/S, which is overestimated by a factor of about 1.5, would be reduced to the value obtained by *Ab initio* calculations.

Calculations of the propagation of the wavepacket in time were carried out using Kosloff's[40,41] time dependent Schrödinger equation integrator program acquired from Professor Dan Imre at the University of Washington. This program has been used in a number of applications[42-44] and is based on the solution of the time dependent Schrödinger equation,

$$-\frac{i}{\hbar}\hat{H}(Q,t)\Psi(Q,t) = \frac{\partial\Psi(Q,t)}{\partial t},$$

where $\Psi(Q,t)$ is the state of the system, $\hat{H}(Q,t)$ is the total Hamiltonian for the system, Q is the spatial coordinate and t is the time coordinate. The advantage of the time dependent approach is that only the initial conditions need to be specified; the state of the system at a later time is calculated by the method. Kosloff's program utilizes the Fourier method to propagate the initial wavefunction in time. The Fourier method is based on the assumption that an arbitrary function f(Q) can be written as a linear combination of a set of

functions, $g_n(Q)$, as

$$f(Q) = \sum_n a_n g_n(Q),$$

where the coefficients a_n are given by the Fourier Transform,

$$a_n = \frac{1}{N}\sum_{n=1}^{N} f(Q_n)e^{-i2\pi nQ/L}.$$

The a_n represent the amplitude of the wavefunction in momentum space. Since the total Hamiltonian can be written and it is

$$\hat{H} = \frac{P^2}{2M} + V(Q),$$

a recipe can be given for finding the value $\hat{H}(Q,t)\Psi(Q,t)$.

(1) Given Ψ, calculate $P^2\Psi$ by a N dimensional Fast Fourier Transform (FFT) of Ψ followed by a multiplication by $(a_{n1}^2 + \ldots + a_{nk}^2)$ and then an inverse FFT

(2) Calculate $V(Q,t)\Psi(Q,t)$, since $V(Q,t)$ is known, and add to the result from step (1) to give $i\hat{H}(Q,t)\Psi(Q,t)$

(3) Calculate $\Psi(Q,t+1)$ from $\Psi(Q,t+1) = \Psi(Q,t-1) - 2i\hat{H}(Q,t)\Psi(Q,t)$

Steps (1) through (3) are then repeated for as many time steps as are desired. The testing of the time integrator program consisted of propagating a gaussian in a harmonic oscillator potential and writing out the function at later times. This problem has been solved exactly and it is known that a displaced gaussian will keep the original shape of the density function, $|\Psi\rangle\langle\Psi|$, also known as the mod squared, at all times. The expectation values for the position, $\langle x\rangle$, and momentum, $\langle p\rangle$, will behave exactly like the classical position and momentum values for a classical oscillator, for example a child on a swing. Running a simulation for the harmonic oscillator case gave gaussians that did not change in

profile, only their positions changed in time, therefore the numerical accuracy of the method was verified.

Graphic displays of the transition densities were obtained using "DISPAN" and "DBAR," programs based on "TNDL5" written by Professor Patrik Callis and Dr. Bruce Anderson, modified to use subroutines in the DISSPLA Library on the node GRAPH on the VAX cluster.. The three-dimensional molecular orbital plots were obtained using a version of Jorgenson's PSI program also adapted to use the subroutines in the DISSPLA library. These adaptations allow for hardcopy output generated on the VAX cluster to be printed on the DEC LN03 ScriptPrinter in the chemistry computerlab (Room 321 Gaines Hall).

RESULTS AND DISCUSSION

Benzene e_{2g} vibronic coupling

Table 2 shows the results of "standard" computational results for the vibronically induced oscillator strengths of the benzene L_b transition for modes ν_6 and ν_8 in both the ground and L_b states, from force field determinations which are expected to have improved accuracy.[45,46] The displacements used for these calculations are shown in Figure 10.

Table 2. INDO/S and CNDO/S calculations of ν_8 and ν_6 induced oscillator strengths in the $^1B_{2u}(L_b)$ excited state of benzene using ground and excited state normal modes[a]

Calculation	Oscillator Strength($\times 10^4$)		Ratio f_6:f_8
	f_{6a}	f_{8a}	
experiment[b]	7	≈0.07	100-200
ground state[c] INDO/S	6.36(6.55)	2.00(1.98)	3.18(3.30)
excited state[d] INDO/S	7.58(7.80)	1.60(1.59)	4.73(4.91)
ground state[c] CNDO/S	6.65(6.94)	2.69(2.70)	2.47(2.57)
excited state[d] CNDO/S	8.23(9.09)	2.04(2.11)	4.03(4.30)

[a] Mataga-Nishimoto electron repulsion integrals and 196 singly excited configurations were used
[b] Refs. 3, 4, 47, 48. Note $f_{6a} = .5(f_{6a} + f_{6b})$
[c] Ref. 45
[d] Ref. 46
[e] Values in parentheses are from the perturbation theory described in the text.

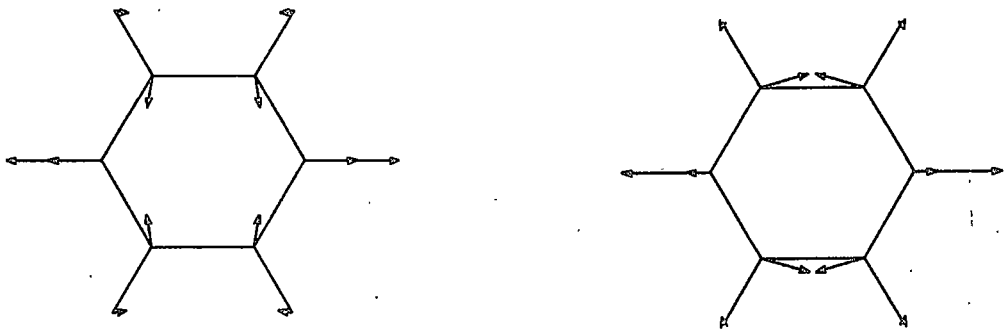

Figure 10. Normal modes ν_6 (left) and ν_8 (right) for benzene.

The calculated ratios for the induced intensity caused by the two e_{2g} modes, f_6:f_8, of about 3 for ground state modes and 5 for excited state modes is similar to earlier results[3] using different force fields.[49] So, while the new modes may be improved from the standpoint of frequency predictions, they show little change in calculations of vibronic coupling strength.

Further investigation of the effect of modes on the coupling ratios was accomplished by doing INDO/S calculations on linear combinations of the ν_6 and ν_8 L_b excited state modes. These calculations show the ratio to be insensitive to mixing up to about 10% relative amplitudes. By mixing nearly equal amounts of ν_6 and ν_8, the ratio f_6:f_8 did approach the experimental value of one hundred. Since it is rather unlikely that the estimates of the normal modes is in such error, the CNDO procedure was examined for the source of the discrepancy.

Table 3 gives the calculated vibronic intensities for ν_6 and ν_8 using a variety of parameters. These results show the strong dependence on the nature of the γ used. Other electron repulsion schemes give much higher ratios of f_6:f_8 than the commonly used MN. The OK γ, which is not normally used with only

Table 3. Comparison of ν_6 and ν_8 induced L_b oscillator strengths from CNDO/S and INDO/S using different sets of parameters.

Number	Type	CI[a]	γ[b]	Oscillator Strength($\times 10^4$)		Ratio f_6:f_8
				f_{6a}	f_{8a}	
1	INDO/S	4 S	MN	4.77(4.83)[c]	1.00(0.98)	4.77(4.91)
2	CNDO/S	4 S	MN	4.21(4.49)	1.03(1.04)	4.20(4.30)
3	INDO/S	196 S	OK	5.57(5.63)	0.219(0.230)	25.4(24.3)
4	INDO/S	4 S	OK	4.28(4.31)	0.166(0.180)	25.8(24.3)
5	CNDO/S	196 S	OK	6.33(5.20)	0.410(0.330)	15.4(15.5)
6	CNDO/S	4 S	OK	4.02(4.25)	0.271(0.270)	14.8(15.5)
7	INDO/S	209 SD	OK	1.77(1.59)	0.100(0.070)	17.7(24.3)
8	INDO/S	50 SDπ	OK	1.75(1.62)	0.096(0.070)	18.2(24.3)
9	INDO/S	196 S	n=2.5	5.27(5.40)	0.032(0.041)	165(133)
10	INDO/S	208 SD	n=2.5	2.04(1.86)	0.036(0.014)	57.0(133)
11	INDO/S	196 S	P1	3.93(3.82)	0.321(0.275)	12.2(13.9)
12	INDO/S	4 S	P1	2.93(2.81)	0.243(0.202)	12.0(13.9)
13	CNDO/S	196 S	P1	4.68(4.38)	0.00223(0.00519)	2100(844)
14	CNDO/S	4 S	P1	3.45(3.30)	0.00167(0.00392)	2060(844)
15	CNDO/S[d]	4 S	P1	5.52(5.28)	0.0170(0.0236)	325(224)
16	INDO/S	196 S	P2	2.81(2.73)	0.026(0.0202)	108(135)

[a] The total number of singly (S) or singly and doubly excited (SD) configurations is given. π means $\pi\pi^*$ configurations only

[b] See text and figures 9 and 11

[c] Values in parenthesis are from the perturbation theory described in the text

[d] Interaction factor (f_π) is .69. f_π = .585 for all other calculations

singly excited configurations because excited state energies are not accurately predicted, gives ratios of f_6:f_8 in the range of fifteen to twenty-five.

Both MN and OK use an interpolation between semiempirical one-center Coulomb repulsion integrals and Coulomb's law in the large distance limit. Both MN and OK have the form

$$\gamma_{AB} = \{R^n + [\frac{1}{2}(\gamma_{AA}+\gamma_{BB})]^{-n}\}^{-1/n},$$

where n=1 for MN and n=2 for OK. The MN curve is displayed in graph form as the curve labeled "MN" in Figure 11. When the value for n is 2.5, as is the case in calculations labeled 9 and 10, the ratio is found to be on the order of the experimental magnitude. Including doubly excited configurations brings predictions of excited state energies to be similar to OK γ. This scheme is labeled "N=2.5" in Figure 11.

Entries 11-15 use a polynomial γ which exploit some well known relationships between energy differences between excited state energies and the γ_{ij}'s along with the observed changes in the diagonal Fock matrix elements. In the e_{2g} vibrations, the diagonal Fock matrix elements change is on the order of 2:−1:−1. This is the same ratio as in the diagonal matrix elements of the transition density between the L_b state and the B_b state. This transition density is shown in Figure 11. It was thought that selecting a γ so that the changes in the diagonal elements of the transition density and the Fock matrix changes would exactly cancel would tune out the vibronic activity on the mode ν_8. Setting a polynomial γ so that $\gamma_{11} - \gamma_{12} - \gamma_{13} + \gamma_{14} = 0$ along with keeping the energy spacings of L_a, L_b, B_a and B_b in agreement with experiment leads to

$$\gamma_{AB} = \frac{1}{2}(\gamma_{AA}+\gamma_{BB}) - .0362R + .003986R^2 + 8.78\times10^{-4}R^3 - 3.4\times10^{-4}R^4$$

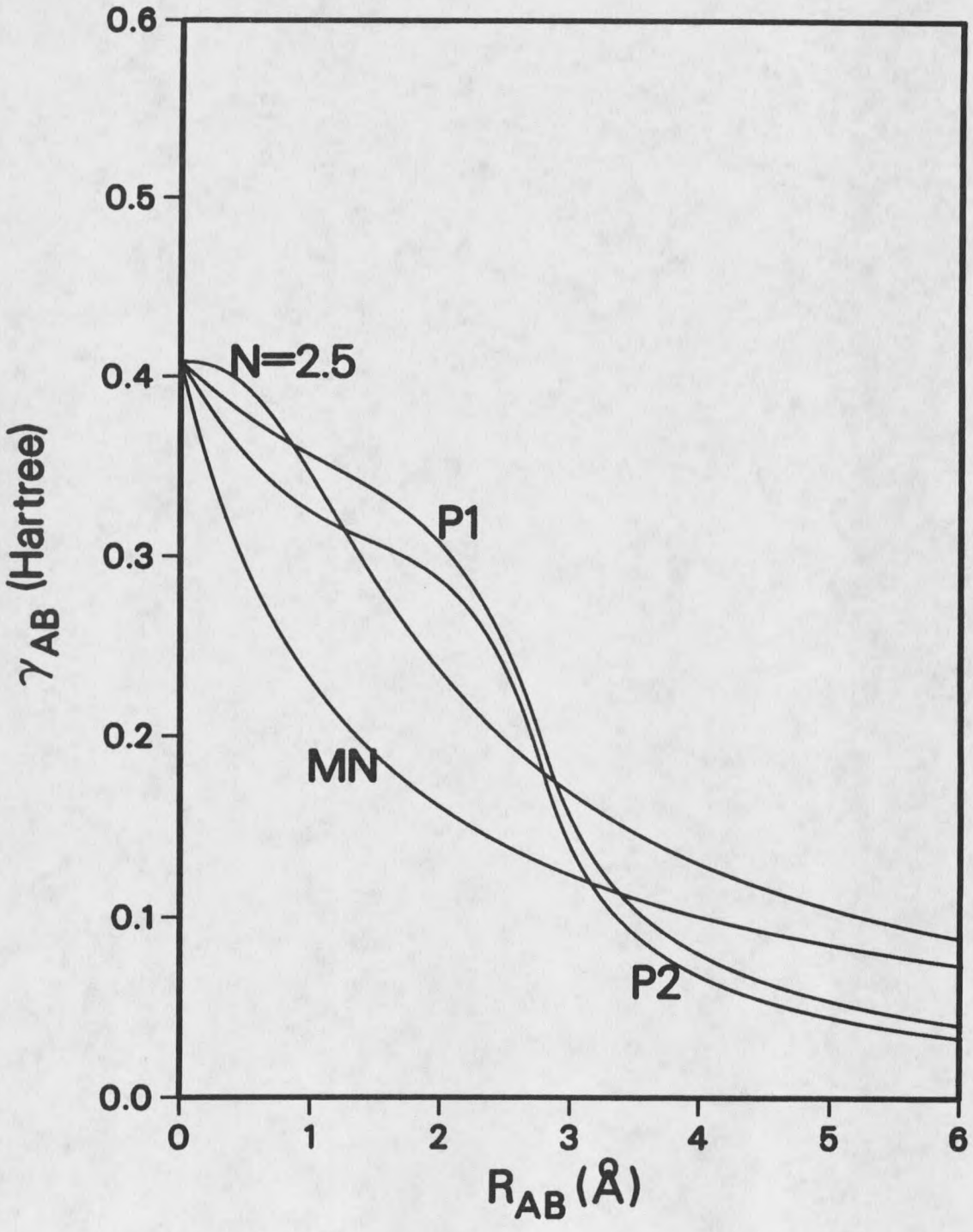

Figure 11. Electron repulsion schemes used in the CNDO and INDO study of vibronic coupling in benzene.

for $R \leq 2.9$Å. At longer distances

$$\gamma_{AB} = \frac{a}{(R-b)},$$

where a and b are picked to match the slope and value of the function. This curve is labeled P1 in Figure 11.

Using this form for γ gives f_8 of nearly zero and the ratio f_6:f_8 of about two thousand. By changing the overlap factor[34] from .585 to .69, the energy of the transitions is in agreement and the ratio f_6:f_8 is about three hundred. Entry 16 in Table 3 gives the results for another polynomial,

$$\gamma_{AB} = \frac{1}{2}(\gamma_{AA}+\gamma_{BB}) - .066072R + .010206R^2 + 1.651\times10^{-3}R^3 - 5.25\times10^{-4}R^4,$$

for $R \leq 2.9$Å. In addition to giving a large ratio f_6:f_8, it also accurately predicts the energy spacings between excited states with INDO/S and 196 configurations. This polynomial γ is represented in Figure 11 by the curve labeled P2.

These results lead to the conclusion that the failure of CNDO/S and INDO/S calculations in predicting the vibronic coupling strengths of the e_{2g} modes in the $^1B_{2u}$ state of benzene lies in the MN electron repulsion scheme, and that its failure rests in the ν_8 coupling which is predicted by MN γ to be large. This result leads to the question, "Why is the weakness of the ν_8 vibronic coupling so sensitive to electron repulsion schemes used?"

The π molecular orbitals for benzene in its equilibrium geometry have the two highest occupied molecular orbitals (HOMO) and lowest unoccupied molecular orbitals (LUMO) as degenerate pairs (orbitals 2, 3, 2′ and 3′ in Figure 1). The L_b ($^1B_{zu}$) state is given by a linear combination of two $\pi\pi^*$ electronic transitions (or configurations), $2 \rightarrow 3'$ and $3 \rightarrow 2'$, both with equal but opposite coefficients of $2^{-1/2}$ and $-2^{-1/2}$, when the orbitals are phased as shown in Figure

1. Both of these configurations contribute equal transition moments and should there be an unequal contribution from these two configurations, a nonzero oscillator strength will result. The larger the difference in the two coefficients, the larger the calculated oscillator strength will be. The factors which contribute to the configuration energy are: 1). Orbital energy difference and, 2). Electron repulsion, or the energy that is required to place an electron in a given orbital due to the repulsion of all the other electrons in the molecule. This is calculated for both orbitals. The equation that determines the configuration energy is

$$E(\chi_i^k) = E(k) - E(i) - (kk|ii) + 2(ki|ik),$$

where E(k) and E(i) are the energies of molecular orbital k and i; (kk|ii) is the Coulomb integral; (ki|ik) is the exchange integral. For the configurations involved in the L_b state, $\chi_2^{3'}$ and $\chi_3^{2'}$, the Coulomb integrals and exchange integrals must be approximately equal at any nuclear configuration, since within the ZDO approximation (ki|ik) is given by $\rho^{ki,ik}:\gamma$, where a matrix element of $\rho^{ki,ik}$ is defined by $\rho_{n,m}^{ki,ik} = \rho_{nn}^{ki}\rho_{mm}^{i\,k}$, (the outer product of the diagonals of the densities). For the exchange integrals, (3′2|23′) and (2′3|32′), the matrices $\rho^{3'2,23'}$ and $\rho^{2'3,32'}$ are equal and $\gamma:\rho^{3'2,23'} = \gamma:\rho^{2'3,32'}$. The Coulomb integrals (3′3′|22) and (2′2′|33) are calculated through the matrices $\rho^{3'3',22}$ and $\rho^{2'2',33}$. These two matrices are transposes of each other and will map identically onto a symmetric matrix, such as γ. Since the molecular orbitals do polarize, there is a difference between the $\rho(Q)$ and $\rho(0)$ upon displacement on the molecule, ρ' is not zero. However, this term is second order and the effect is small compared to the shifting of orbital energies. Thus, for the configurations $\chi_2^{3'}$ and $\chi_3^{2'}$ the configuration energy differences can be written as

$$\Delta E(\chi) = E(3') - E(2') + E(3) - E(2).$$

To first order, a molecular orbital energy can be written $E(\varphi_i) = E°(\varphi_i) + \rho^{\varphi i \varphi i}:F'$, where F' is the change in the Fock matrix brought about by the distortion of the molecule and $E°$ is the molecular orbital energy at the equilibrium geometry. Using this in the equation for energy differences gives

$$\Delta E(X) = E°(3') - E°(2') + E°(3) - E°(2) + [\rho^{3'3'} - \rho^{2'2'} + \rho^{33} - \rho^{22}]:F'.$$

The terms from the zeroth order contribution give zero, since $3'$ and $2'$ are degenerate as are 3 and 2, leaving $\Delta E(\chi) = [\rho^{3'3'} - \rho^{2'2'} + \rho^{33} - \rho^{22}]:F'$. The term in square braces is equal to $\rho^{Lb,Bb}$, the transition density between the forbidden L_b state and allowed B_b state in benzene.[22] Figure 12 shows this transition density in position space. Thus, the mixing of the forbidden L_b state with the allowed B_b state is a direct result of the loss of degeneracy in the HOMO and LUMO pairs. For benzene, ν_{6a} and ν_{8a} are expected to induce intensity to the L_b state almost exclusively by mixing with the $E_{1u}(B_b)$ state at about 180 nm, giving the induced oscillator strength of

$$f_{Lb}(Q) = \left(\frac{H'_{Lb,Bb}}{[E°_{Lb} - E°_{Bb}]} \right)^2 \times \frac{E°_{Lb}}{E°_{Bb}} \times f°_{Bb},$$

where the $E°$ and $f°$ are the undistorted molecule values for the state energies and the B_b oscillator strength.

What now is needed is an expression to relate $F':\rho^{LbBb}$ to $H'_{Lb,Bb}$. CNDO/S and INDO/S calculate states by a linear combination of configurations giving a state Ψ_K by,

$$\Psi_K = \sum_\kappa d_{K\kappa}\chi_\kappa,$$

where χ_κ is a configuration resulting from taking an electron out of orbital i and placing it in orbital j. The configuration χ_κ is known as a singly excited configuration.

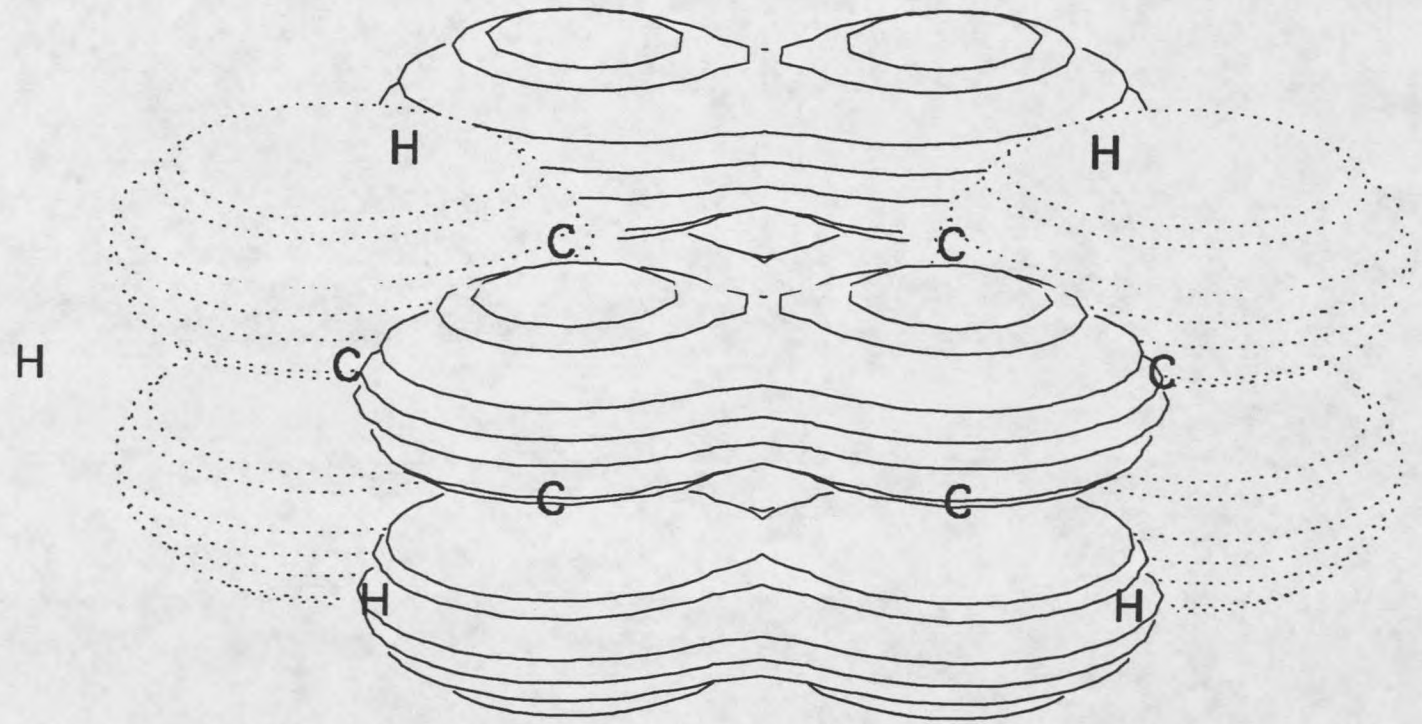

Figure 12. The transition density between the L_b and B_b states in benzene.

If only singly excited configurations are considered, then the matrix element H_{KL} is given by $\langle\Psi_K|H|\Psi_L\rangle$, and since the states can be written as a linear combination of configurations, the states also can be expressed this way. The H_{KL} element is,

$$H_{KL} = \sum_{\kappa}\sum_{\lambda} d_{K\kappa}d_{L\lambda}\langle\chi_\kappa|H|\chi_\lambda\rangle,$$

where κ implies an excitation from molecular orbital i to molecular orbital j and λ implies an excitation from molecular orbital k to molecular orbital l.

This gives H_{KL} between singly excited configurations as,[35]

$$H_{KL} = \sum_{\kappa,\lambda}[F_{jj} + F_{ll} - F_{ii} - F_{kk} + F_{jl}\delta_{ik} - F_{ik}\delta_{jl} + 2(ij|kl) - (ik|jl)]d_{K\kappa}d_{L\lambda}.$$

This gives

$$H_{KL} = \sum_{\kappa,\lambda}[F:(\rho^{ij} + \rho^{ll} - \rho^{ii} - \rho^{kk} + \rho^{jl}\delta_{ik} - \rho^{ik}\delta_{jl}) + (2\rho^{ij,kl} - \rho^{ik,jl}):\gamma]d_{K\kappa}d_{L\lambda}.$$

Taking the derivative with respect to Q gives H'_{KL} as

$$H'_{KL} = \sum_{\kappa,\lambda}[[F':(\rho^{ij} + \rho^{ll} - \rho^{ii} - \rho^{kk} + \rho^{jl}\delta_{ik} - \rho^{ik}\delta_{jl}) +$$

$$F:(\rho^{ij} + \rho^{ll} - \rho^{ii} - \rho^{kk} + \rho^{jl}\delta_{ik} - \rho^{ik}\delta_{jl})' +$$

$$\gamma':(2\rho^{ij,kl} - \rho^{ik,jl}) + \gamma:(2\rho^{ij,kl} - \rho^{ik,jl})'](d_{K\kappa}d_{L\lambda})$$

$$+ [F:(\rho^{ij} + \rho^{ll} - \rho^{ii} - \rho^{kk} + \rho^{jl}\delta_{ik} - \rho^{ik}\delta_{jl}) + \gamma:(2\rho^{ij,kl} - \rho^{ik,jl})](d_{K\kappa}d_{L\lambda})'.$$

The changes in d do not contribute since states K and L are orthogonal, that is they are not mixed for undisplaced benzene. Of the four remaining terms in this sum, terms two and four are small. These two terms are projections of the change in the transition density on the totally symmetric F matrix and the γ matrix is mapped onto $\rho^{ij,kl}$. Since the change in the transition density matrix is small in this case and shows the 2:-1:-1 ratio for the diagonal elements, the overlap is also small. The third term is the result of the change in the electron repulsion due simply to the change in distance between the atomic centers. This

change can overlap onto the transition density, however, the changes studied in the course of this work have been small in comparison to the changes caused by the first term. Therefore, the Fock matrix change mapped onto the transition density gives a good approximation for H'_{KL} in this case.

Using this formula along with the corresponding F′ for Q along ν_6 and ν_8 and the E°_{Lb}, E°_{Bb} and f°_{Bb} values for each of the CNDO/S and INDO/S calculations gives the results shown in parenthesis in Tables 2 and 3. Agreement with directly calculated values is excellent except where doubly excited configurations are used where errors on the order of 50% are observed.

Fock matrix changes with nuclear distortion show why the ν_8 coupling can become weak. Table 4 shows changes in the Fock matrix corresponding to the P1 γ (calculations 13 and 14 in Table 3), and Table 5 shows the transition densities between four π molecular orbitals, ρ^{22}, ρ^{33}, $\rho^{2'2'}$ and $\rho^{3'3'}$. In order for CNDO/S or INDO/S to eliminate vibronic coupling in ν_8, the value for $\Delta E(\chi)$ has to be zero. One way for this to occur is $\rho^{3'3'}$:F′ + ρ^{33}:F′ = 0 and $\rho^{2'2'}$:F + ρ^{22}:F = 0. This is not the only scenario that will eliminate ν_8 coupling, but the patterns seen in the density matrices suggest using these two constraints. The first constraint, $\rho^{3'3'}$:F′ + ρ^{33}:F′ = 0, leads to F'_{22}=F'_{26}, while the second constraint, $\rho^{2'2'}$:F′ + ρ^{22}:F′ = 0, leads to $2F'_{11} + F'_{22} + F'_{26} - 4F'_{13} = 0$. Combining the two equations, along with the observation that calculations of the e_{2g} modes always gives $F'_{11} = -2F'_{22}$, leads to $F'_{22} = 2F'_{13}$. These relationships between the elements in the change of the Fock matrix show that the change in the F'_{22} element has to be the same sign and twice the magnitude of the C_1-C_3 interaction change. The Fock matrix change caused by ν_8 using P1 γ has this property, while the change using MN γ shows the sign of F'_{22} to be opposite of F'_{13}. Using OK γ gives F'_{22} to be the same sign as F'_{13} but smaller in magnitude.

Table 4. Fock matrix changes caused by ν_{6a} and ν_{8a} distortions using P1.

F'_{8a}						
-0.95						
2.83	0.45					
-0.25	-5.71	0.45				
1.68	-0.25	2.83	-0.95			
-0.25	-0.86	0.49	2.83	0.45		
2.83	0.49	-0.86	-0.25	-5.71	0.45	
F'_{6a}						
0.61						
-0.67	-0.32					
0.55	1.45	-0.32				
-1.78	0.55	-0.67	0.61			
0.55	0.93	-1.12	-0.67	-0.32		
-0.67	-1.15	0.93	-0.55	1.45	-0.32	

The mode ν_6 is primarily bending, and so has large changes in the next-nearest-neighbor positions relative to the diagonal changes, making the constraints in the Fock matrix changes unobtainable for ν_6. The ν_8 near-neighbor changes though large do not contribute anything to the analysis here because the density matrix elements for ρ^{33} and $\rho^{3'3'}$ are of opposite sign in the near-neighbor positions. From the point of view of orbital energies, there has to be an equal change in the energies of the orbitals that make up the HOMO pair and the LUMO pair for the ν_8 coupling to vanish. ν_8 is largly a C_2-C_3 stretching mode and noting from the molecular orbitals in Figures 1 and 2, the node between these two atomic centers in orbital 2 indicates that displacement along this mode will destabilize orbital 2 because the atoms C_2 and C_3 are now closer together. The opposite is true for molecular orbital 3 where the coefficients on C_2 and C_3 have the same sign. Looking at the pattern in molecular orbitals 2′ and 3′, a similar pattern is seen except now 2′ is a bonding molecular orbital between C_2 and C_3 and orbital 3′ is antibonding between C_2 and C_3. Only when the

Table 5. Transition density matrices between orbitals 2, 3, 2′ and 3′.

$12\rho^{2,2}$						
4						
2	1					
-2	-1	1				
-4	-2	2	4			
-2	-1	1	2	1		
2	1	-1	-2	-1	1	
$4\rho^{3,3}$						
0						
0	1					
0	1	1				
0	0	0	0			
0	-1	-1	0	1		
0	-1	-1	0	1	1	
$12\rho^{2',2'}$						
4						
-2	1					
-2	1	1				
4	-2	-2	4			
-2	1	1	-2	1		
-2	1	1	-2	1	1	
$4\rho^{3',3'}$						
0						
0	1					
0	-1	1				
0	0	0	0			
0	1	-1	0	1		
0	-1	1	0	-1	1	

magnitudes of the changes in orbital energies are identical for all four orbitals will ν_8 be "tuned out", or the oscillator strength caused by ν_8 will be zero. Table 6 shows this effect for P1 and MN with both mode ν_6 and mode ν_8. Figure 13 gives a pictorial view of the energy changes caused by these modes when MN γ is used and Figure 14 shows the energy changes for the modes when P1 γ is used.

Table 6. Molecular orbital energies and energy shifts caused by the e_{2g} modes in benzene in Hartrees.

			$F':\rho^{ii}$			
ν	γ	E°	2	3	2′	3′
6	MN	-.0251	-.0020	.0021	-.0000	.0001
8	MN	-.0251	.0054	-.0055	-.0046	.0046
6	P1	.4562	-.0013	.0013	-.0003	.0003
8	P1	.4562	.0048	-.0049	-.0048	.0048

It was surprising that these changes in the diagonal elements occurred. Since they did occur, their importance had to be considered in understanding the mechanism of the e_{2g} vibronic coupling. The change in diagonal matrix element is given by

$$F'_{rr} = -\frac{1}{2}P'_{rr}\gamma_{AA} + \sum_B P'_B\gamma_{AB} + \sum_B (P_B - Z_B)\gamma'_{AB},$$

where P_{rr} is the electron density element for the r^{th} basis orbital and P_B is the sum of electron densities for the basis orbitals on atom B. The first two terms of the equation contain the change in electron density on a given atom B and the change in basis orbital r, while the third term carries the effect of moving atomic centers to and fro with their electrons following them perfectly. The first two terms dominate in this case. Previous studies[10,51,52] have used a similar formal treatment, however, these studies have kept electron densities constant and only considered the third term, which is the effect of changing the relative positions of nuclei while the electrons follow them. The results of this study show that mapping the change in nuclear positions onto the transition density pattern reduces the value of the second term in the equation. The total atomic electron density changes that CNDO/S gives for modes ν_{6a} and ν_{8a} are presented in Figure 15. The magnitude of the changes is proportional to the diameter of the

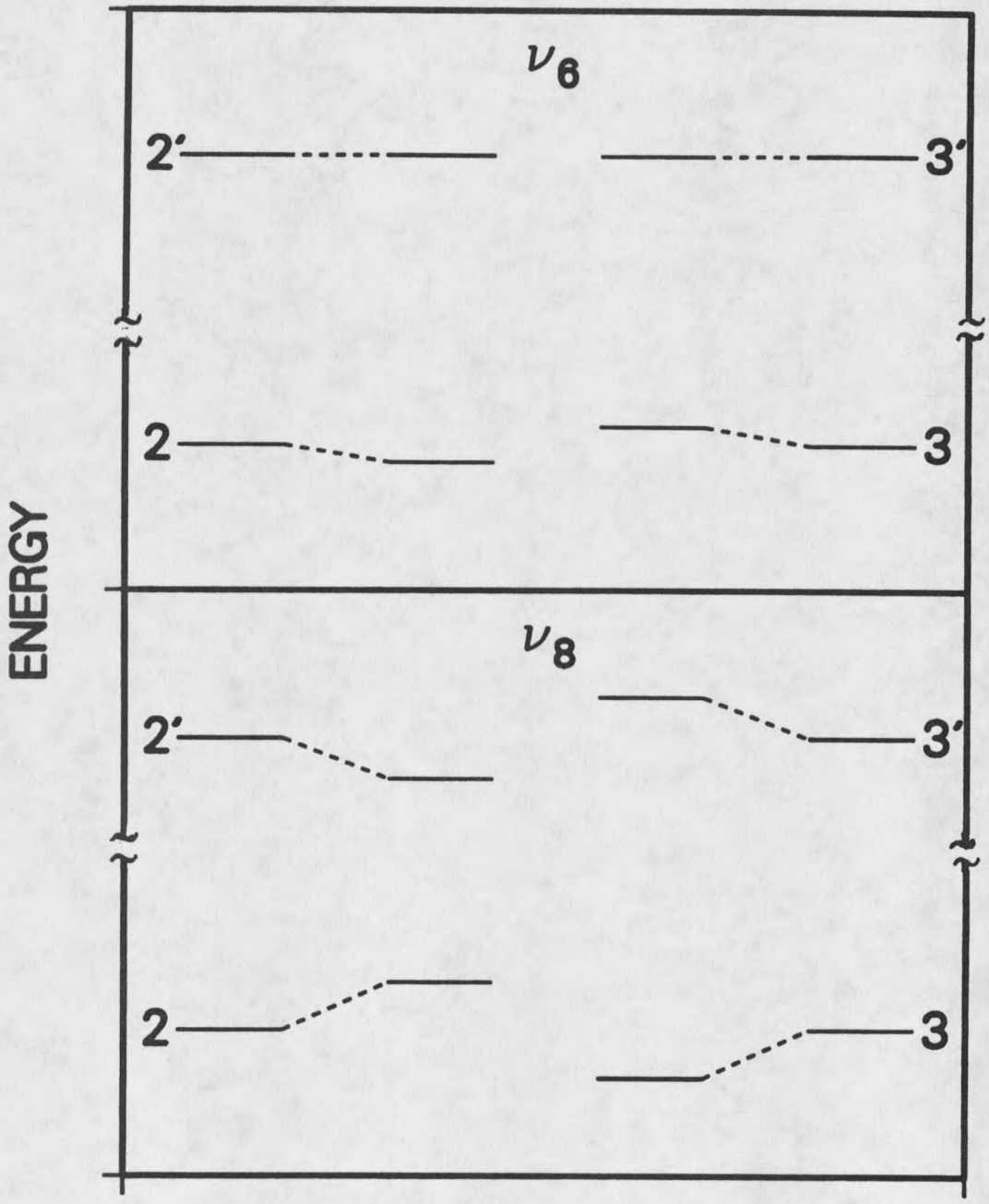

Figure 13. Orbital energy changes caused by normal modes ν_6 and ν_8 using MN γ's

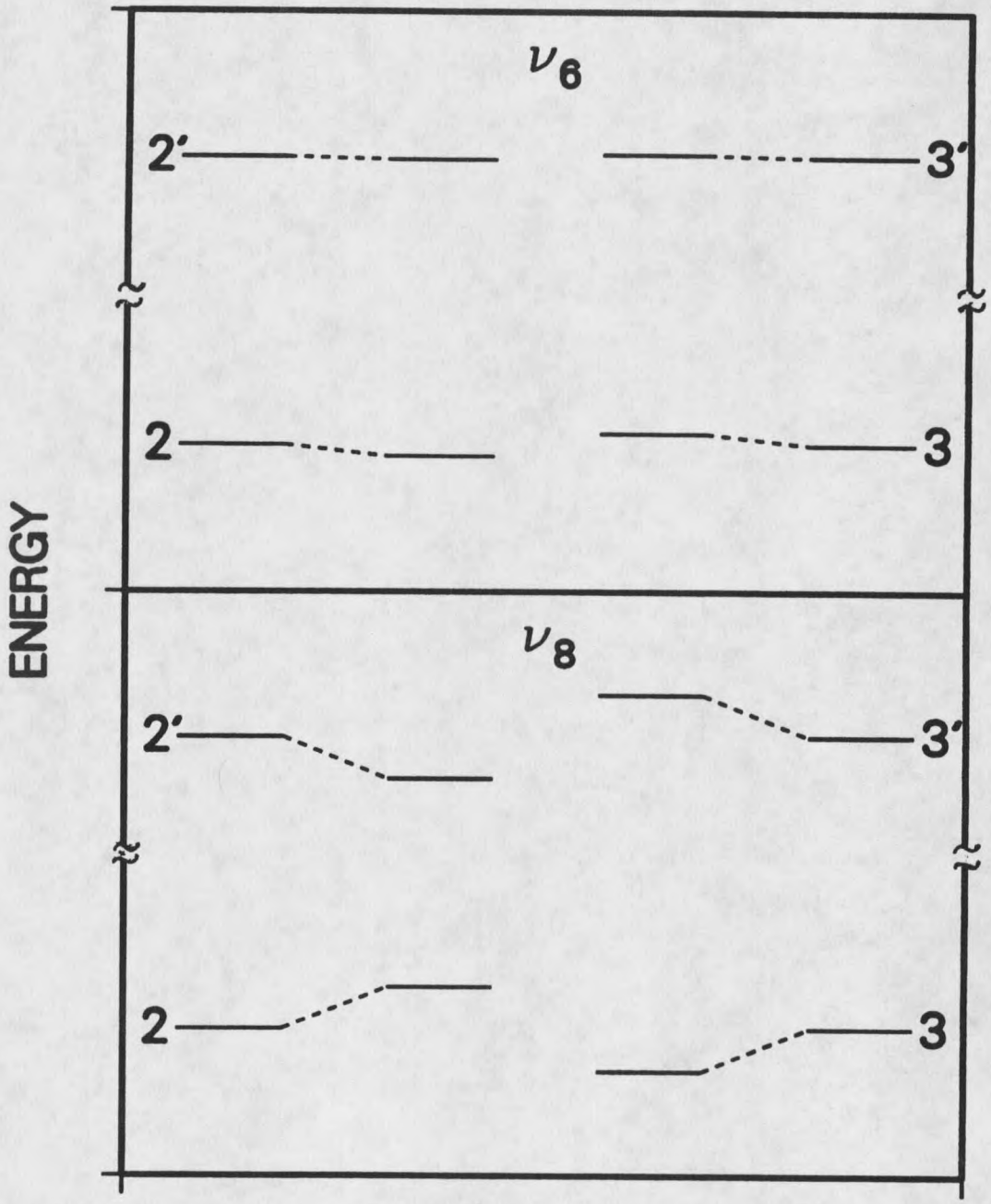

Figure 14. Orbital energy changes caused by normal modes ν_6 and ν_8 using P1 γ's

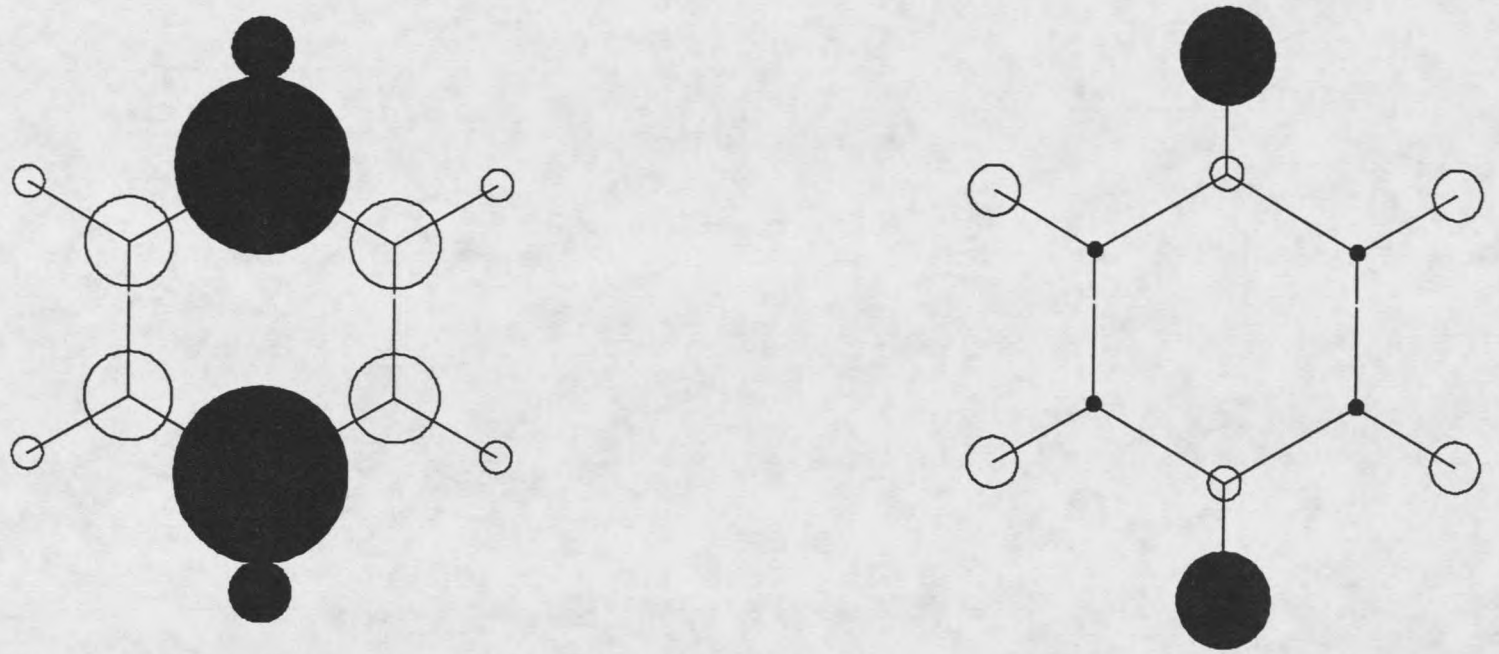

Figure 15. Charge density changes caused by normal modes ν_6 (left) and ν_8 (right).

circles shown at each center with white and black colors signifying an increase and decrease respectively. The observed pattern of density changes on the carbons of 2:-1:-1:2:-1:-1 is helpful in revealing the reason for the sensitivity of the ν_8 coupling to the γ used, making the different γs map onto the values for $F'_{rr}(Q)$. The changes in the diagonal Fock matrix elements now reflect the electron density changes, this means that a negative change in the diagonal Fock matrix element corresponds to an increase in electron density in that orbital. In the case of the MN γ, the term due to electron repulsions from the other atomic centers in the molecule was larger than the term due to the electron repulsion for the other electron on that center and caused the diagonal Fock matrix changes to be positive on atomic centers that gained electron density. This specific pattern of electron density changes may only apply at the CNDO level, however, the concept of electron density changes may survive any level of theory.

The second excited state in benzene, termed L_a, is made up of the complementary configurations $\chi_3^{3'}$ and $\chi_2^{2'}$ and has B_{1u} symmetry. The effects of normal modes ν_8 and ν_6 are also complementary, so ν_8 exhibits strong vibronic coupling in the L_a state where ν_6 is much weaker. Another normal motion, ν_9, which is similar to ν_8 with large H motions instead of C motions, is also vibronically active in the L_a absorption.[53] The calculations listed in Table 7 give an account of the effect of ν_9 vs. ν_6 in the L_a state using Albrecht's modification of normal displacements given by Whiffen.[54,55] Also included in Table 7 are calculations using normal modes for the ground and L_b states calculated by Goodman et al.[45,46] Table 7 also includes the results of calculations on the normal modes generated by Guo and Karplus[56] using *Ab initio* force fields from Hartree-Fock/6-31G* basis and second order MP perturbation theory with a 6-31G basis.

Table 7. Results of INDO/S calculations on the benzene L_a state

Mode	f_{La}	$C_2 - C_3$ Bond Length Change (Å)
Whiffen ν_6	.014	.0103
Whiffen ν_8	.034	.0179
Whiffen ν_9	.013	-.0083
Goodman XS ν_6	.005	.0053
Goodman XS ν_8	.058	-.0276
Goodman XS ν_9	.014	.0113
Goodman GS ν_6	.002	.0026
Goodman GS ν_8	.052	-.0246
Goodman GS ν_9	.019	.0128
HF/6-31G* ν_6[a]	.003	.0039
HF/6-31G* ν_8	.049	-.0238
HF/6-31G* ν_9	.012	.0106
MP2/6-31G ν_6[b]	.003	.0039
MP2/6-31G ν_8	.051	-.0250
MP2/6-31G ν_9	.012	.0108

[a] Normal modes from Guo and Karplus based on HF/6-31G* *Ab initio* force fields

[b] Normal modes from Guo and Karplus based on MP2/6-31G *Ab initio* force fields

The ratio f_6:f_9 is extremely sensitive to the displacement used. A closer look reveals that the C-C bond length changes also listed correlate well with the size of the coupling intensity. The transition density between the L_a state and the allowed B_a state is shown in Figure 16. This transition density has large elements in the bonds between C_2 and C_3,[57] and the calculated intensity is expected to be proportional to the square of the change in the off-diagonal Fock matrix element between those two centers, which is proportional to the change in the bond length.

It is curious that the total oscillator strength does not appear to be conserved through the series of calculations of the induced oscillator strength in the L_a state as might be expected. This may be related to the fact that the dependence on the square of the C_2-C_3 bond length change is not linear with

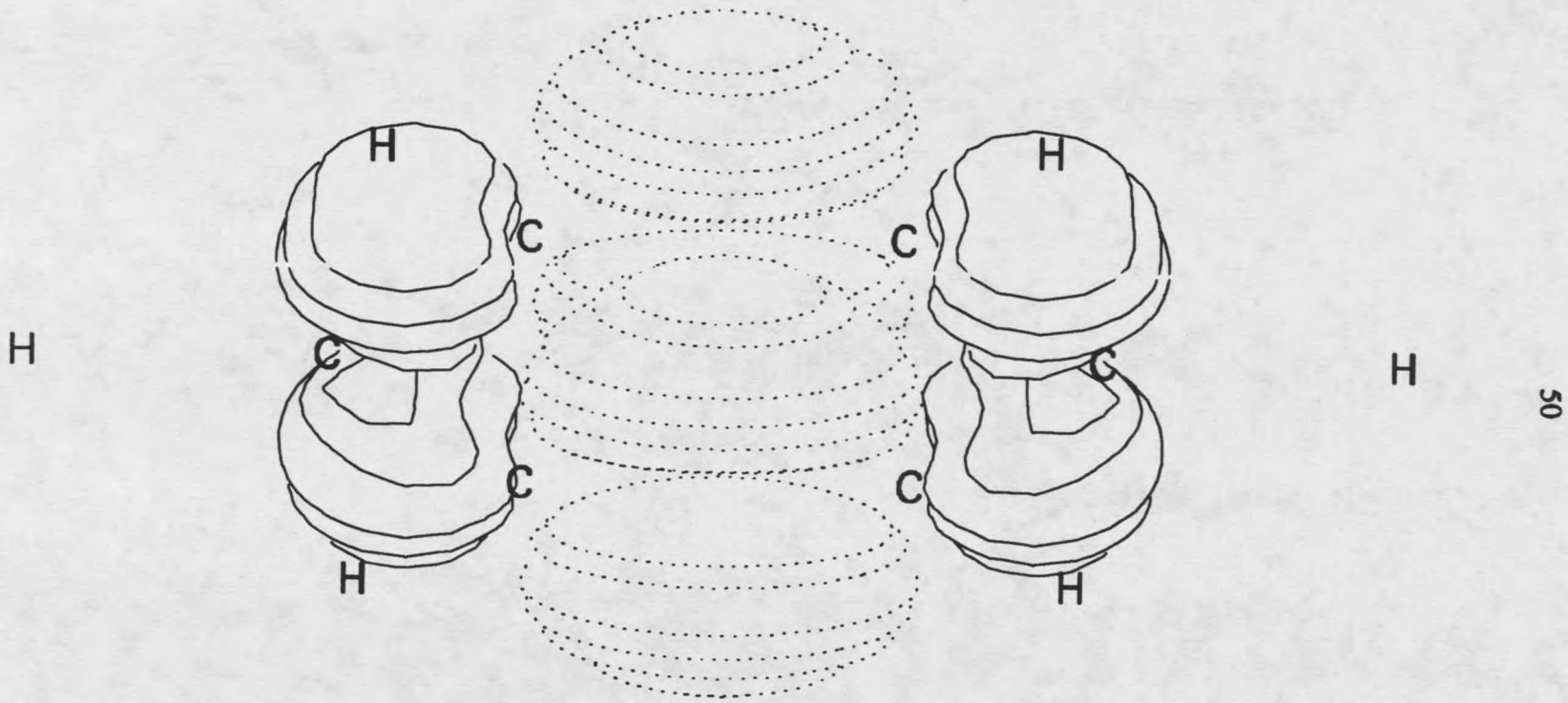

Figure 16. The L_a B_a transition density in benzene.

distance change along the C_2-C_3 bond. If the bond length changes between sets of modes are considered, it can be seen that in the Goodman modes the magnitude of the total C_2-C_3 bond length change for mode ν_8 is larger than in the Whiffen modes. On the other hand, the Whiffen modes contain a larger C_2-C_3 bond length change in mode ν_6.

The Guo-Karplus modes also predict the mode ν_9 to be more effective in inducing vibronic coupling activity in the L_a state than mode ν_6, as is seen in the final six entries in Table 7. The pattern in these modes also shows that the change in the C_2-C_3 bond length squared is well correlated with the calculated oscillator strength for the mode.

Applying the perturbation theory from the L_b vibronic coupling study gives qualitative agreement with directly calculated results. However, the L_a state lies much closer to the allowed B states and the mixing is much stronger due to the fact that the L_a state has the same pseudoparity as the B states. Therefore, this situation is not expected to be described in a quantitative way by perturbation theory.

Qualitative agreement is seen, for example, the ratio for modes ν_6 and ν_8 using the perturbation theory developed here can be compared to the CNDO/S calculated ratios. It is found that using the P1 γ's and only 4 excited configurations, along with Goodman's excited state modes differs with the perturbation theory value of approximately 48:1 while the CNDO/S value is about 13:1.

Benzene b_{2u} vibronic coupling

In the two-photon spectrum of benzene, the b_{2u} mode ν_{14} is the dominant mode that induces vibronic coupling.[58] The mechanism by which this mode induces is not clear. Friedrich and McClain[9] attributed the intensity to ground state coupling; Metz,[10] on the other hand, neglects ground state coupling in his analysis. He states that it is the breakdown of Albrecht's selection rule[48] that allows the b_{2u} mode to be seen.

The mode ν_{14} also exhibits the unusual property that it has a higher frequency in the $^1B_{2u}$ state than in the ground state, even though the $^1B_{2u}$ state has a smaller bond order between the carbons in the ring. This pseudo Jahn-Teller effect can be readily explained by ground state coupling to the $^1B_{2u}$ state.[59] The explanation is that the surfaces of the two states when they interact repel each other and this repulsion causes a larger separation than would be seen without the interaction. This separation is depicted in Figure 17 where the dashed curves represent undisplaced two harmonic oscillators of equal frequency and the solid curves are linear combinations of the upper and lower dashed surfaces with a coupling that is linear in the displacement.

If benzene is constrained to remain planar in the $^1B_{2u}$ state, then a b_{2u} mode, of which there are only two, or a combination of planar modes that multiply to give B_{2u} symmetry in D_{6h} will be necessary to promote internal conversion from the $^1B_{2u}$ state to the ground state which is $^1A_{1g}$. This possibility is very intriguing in considering the "Channel Three" phenomenon, the sudden reduction of fluorescence intensity in benzene when the excitation light is roughly

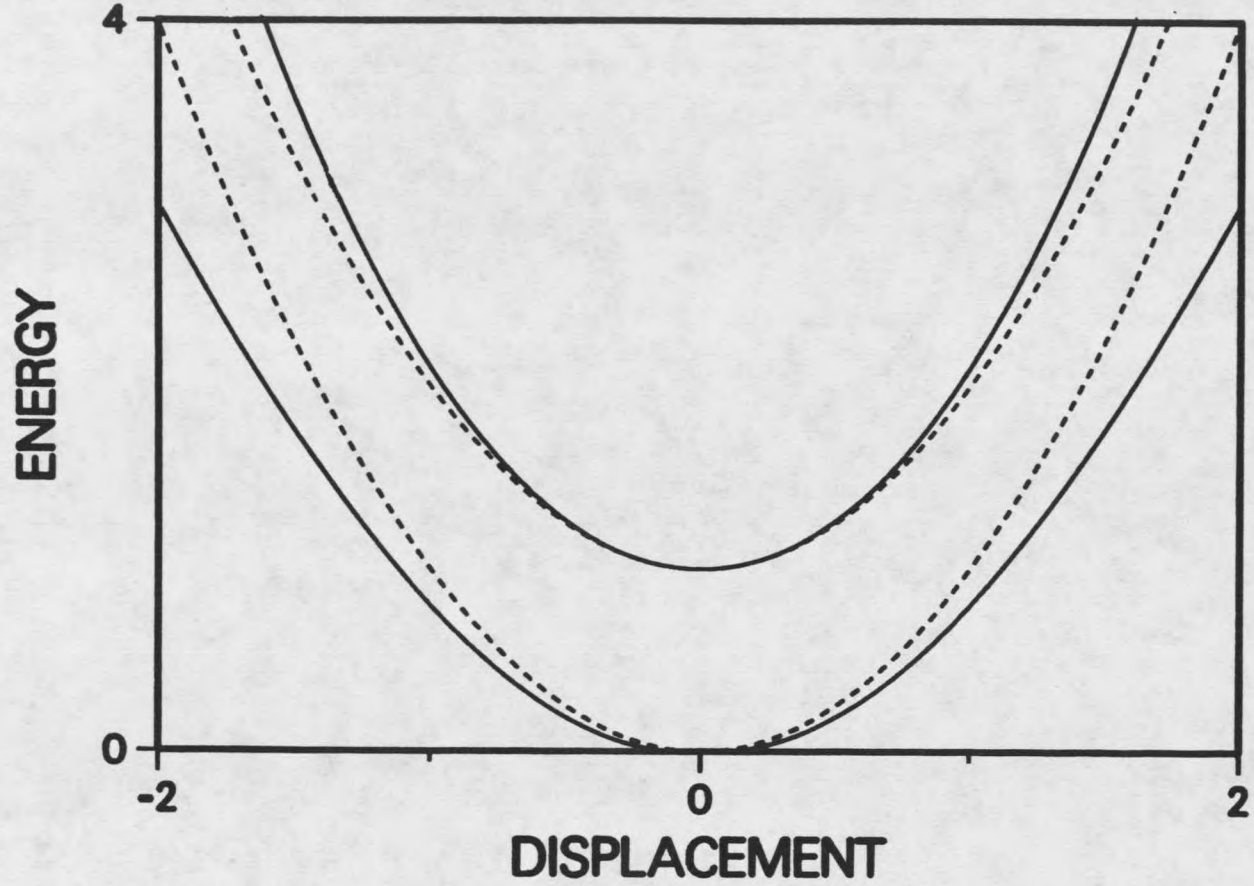

Figure 17. Two harmonic oscillator potentials (dashed lines) and the same two potentials coupled by a linear coupling term.

3000 cm^{-1} above the threshold for L_b absorbance. The term "Channel Three" was coined by Calloman[60] nearly twenty years ago. The search for an explanation of this effect has been the subject of ongoing experimental[61-72] and theoretical[73-76] study. None of these studies has implicated the ν_{14} vibronic coupling in this process. Hornburger and Brand identify the out of plane mode ν_4 as a likely candidate for an accepting mode. Kato[76] considered the prefulvene geometry in benzene to explain "Channel Three". His model, however, traps the molecule in the prefulvene geometry and does not allow the system to return to the excited electronic state.

If the perturbation theory is used to explain the one-photon intensity of the e_{2g} modes, then it is conceivable that the same treatment could shed some light on these questions as well.

The benzene b_{2u} normal mode ν_{14} is depicted in Figure 18, and the changes to the Fock matrix elements, caused by this displacement, are given in Table 8. The changes in the near-neighbor elements dominates those of the other positions, reflecting the alternate stretch-compression action of this mode on the molecule. Table 9 depicts the orbital energies for the undisplaced molecule, the first order energy correction ρ^{ii}:F′ and the orbital energies for the displaced molecule.

Table 8. Fock matrix changes caused by the ν_{14} distortion.

$F'_{14} \times 10^4$ Hartrees					
-0.02					
-9.09	-0.02				
0.00	9.20	-0.02			
-0.20	0.00	-9.09	-0.02		
0.00	-0.20	0.00	9.20	-0.02	
9.20	0.00	-0.20	0.00	-9.09	-0.02

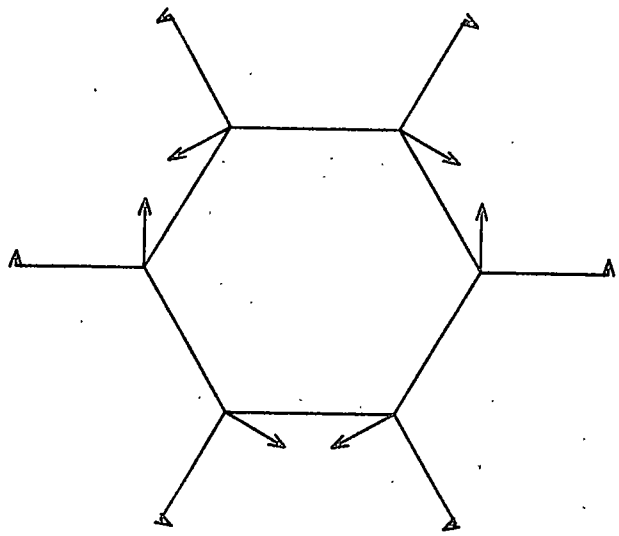

Figure 18. Normal mode ν_{14} in benzene.

Table 9. Orbital energies and first order corrections in Hartrees.

MO	Undisplaced Energy	Correction	Displaced Energy
2	-0.3241	0.0002	-0.3246
3	-0.3241	0.0002	-0.3246
2′	0.0251	-0.0003	0.0256
3′	0.0251	-0.0003	0.0256

It is clear that here the first order change, being quite small and uniform on both pairs of the degenerate orbitals is opposite in sign to the changes that occur when the INDO/S calculation is carried out. Thus, just looking at the first order changes to the molecular orbital energies does not accurately reflect the effect this mode has on the electronic states of benzene. The second order correction, resulting from the interaction between molecular orbitals is given by $F':\rho^{ij}$. For the mixing of molecular orbitals 3 and 2′ the interaction has a value of .0158. The interaction is -.0158 for the mixing of molecular orbitals 2 and 3′. Setting up a 2×2 determinant using the molecular orbital energies with the first order

correction as well as the interaction between the molecular orbitals gives, in Hartrees,

$$\begin{vmatrix} -0.3239 & 0.0158 \\ 0.0158 & 0.0248 \end{vmatrix}.$$

Solving the set of equations gives the energies for molecular orbitals 2 and 3 of −0.3246 a.u. and energies for molecular orbitals 0.0255 a.u. The new molecular orbitals can be expressed as a linear combination of the undisplaced molecular orbitals. The new molecular orbitals are:

$$\varphi_3^n = .9990\ \varphi_3 - .0452\ \varphi_{2'}$$

$$\varphi_{2'}^n = .9990\ \varphi_{2'} + .0452\ \varphi_3$$

$$\varphi_2^n = .9990\ \varphi_2 + .0452\ \varphi_{3'}$$

$$\varphi_{3'}^n = .9990\ \varphi_{3'} - .0452\ \varphi_2.$$

The configuration $\chi^{2'n}_{3\ n}$ can also be written as a linear combination of the χ_i^j's. Using the configuration interaction coefficients, the $^1B_{2u}$ state (L_b) is given by,

$$L_b^n = \frac{1}{\sqrt{2}}(\chi^{3'n}_{2\ n} - \chi^{2'n}_{3\ n}),$$

and

$$L_b^n = \frac{1}{\sqrt{2}}[.9980(\chi_2^{3'} - \chi_3^{2'}) + .0903\chi_G + .04515(\chi^{2'2'}_{3\ 3} - \chi^{3'3'}_{2\ 2}),$$

when the molecule is displaced along ν_{14}.

The term χ_G is the undisplaced ground state. The terms $\chi^{2'2'}_{3\ 3}$ and $\chi^{3'3'}_{2\ 2}$ are doubly excited configurations. The doubly excited configurations result from promotion of two electrons from occupied orbitals to virtual orbitals and contribute to the two-photon intensity by mixing the L_b state to an allowed A_{1g} state that is predicted by INDO/S to occur at about 90,000 cm^{-1}. This state reduces the total calculated two-photon intensity through interference, that is it

adds to the transition tensor of opposite sign from the tensor induced by ground state coupling to the L_b state. This mixing of the orbitals involved in the configurations that are involved in the L_b state directly couples the ground state and the L_b state. The energy changes caused by this mixing of the molecular orbitals are depicted in Figure 19.

A similar calculation to the one in which the molecular orbitals were considered can be done taking the undisplaced ground and L_b states to be basis states, and assuming the interaction between the states to be $F':\rho^{GLb}$ gives a predicted energy separation of 38,516 cm^{-1} by solving the 2×2 equation. This is compared to 36,060 cm^{-1} calculated by CNDO for undistorted benzene and 36,320 cm^{-1} for ν_{14} displaced benzene. These results show the effect of the normal mode ν_{14} to mix or couple the ground electronic state and L_b state, that is, when benzene is displaced along ν_{14} the ground state has an amount of B_{2u} character, and a $^1B_{2u}$ state that has A_{1g} character.

This coupling can show itself two ways: First, it will create a transition dipole between the forbidden L_b state and allowed B state through HT coupling, second, it will allow for a radiationless pathway between the L_b state and the ground state by BO breakdown coupling. The dipole between the L_b and B state is reflected in the two-photon intensity induced by ν_{14}. The two-photon absorption probability is given by,[77]

$$P_{abs} = |\hat{e}_i(R)\cdot S(r)\cdot \hat{e}_i(R)|^2,$$

where $\hat{e}_i(R)$ represents the electric field vector of the incident light, R = X,Y,Z. The matrix S(r) is the two–photon transition tensor, r = x,y,z. An element of S is given by,

$$S_{\alpha\beta} = \sum_n \left[\frac{\langle g|\alpha|n\rangle\langle n|\beta|f\rangle + \langle g|\beta|n\rangle\langle n|\alpha|f\rangle}{E_n - \hbar\omega} \right]$$

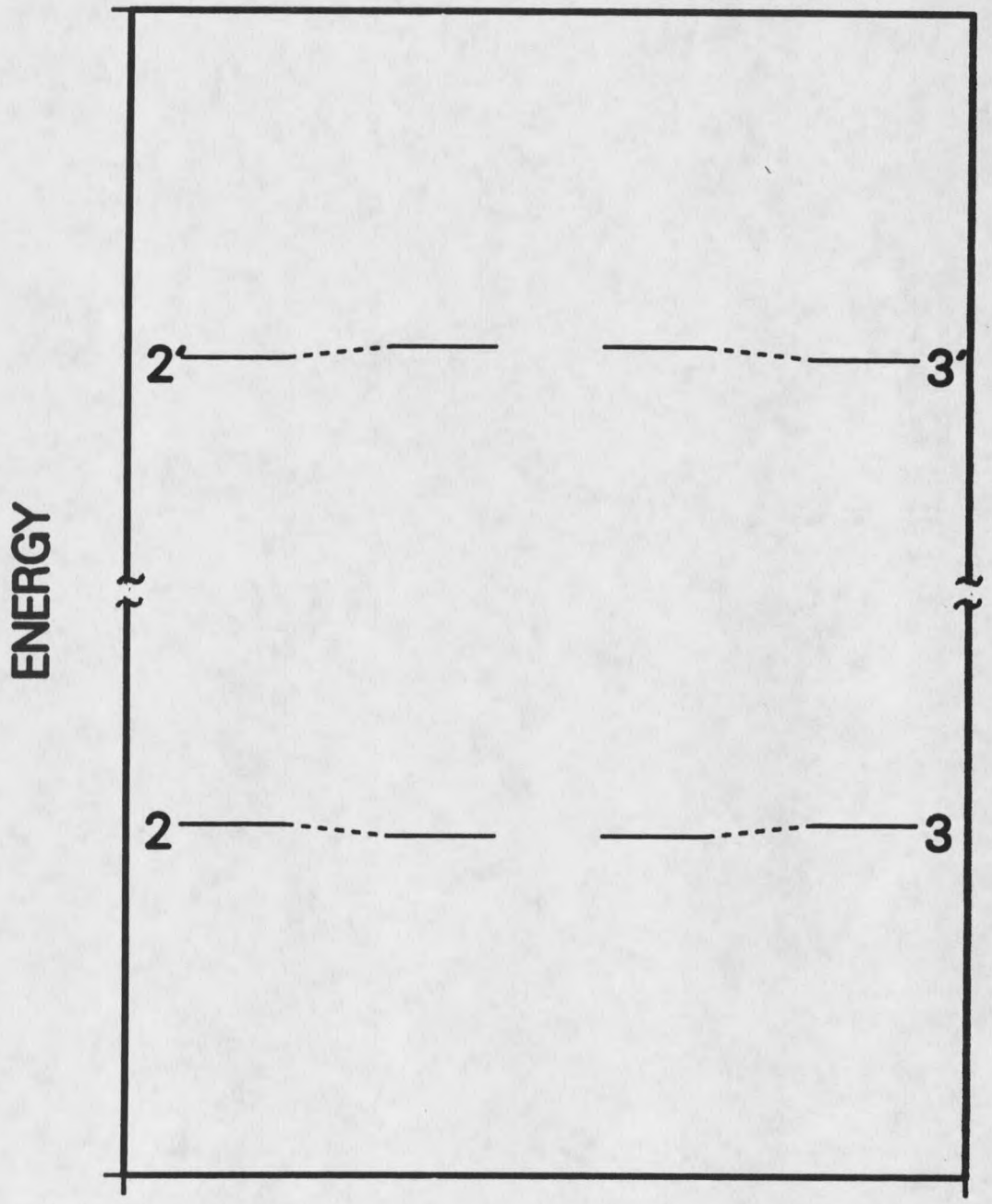

Figure 19. Orbital energy changes caused by normal mode ν_{14} using MN γ's

for α and β = x,y and z. If the benzene L_b state is induced by coupling to the ground state, the only transition tensor elements that will be nonzero are the S_{xx} and S_{yy}. The $S_{\alpha\alpha}$ term in the transition tensor represents two photons being absorbed along the same transition moment direction. Table 10 gives the calculated S_{xx} and S_{yy} transition tensor element for benzene displaced along ν_{14} at several fractions of the root-mean-square displacement. The results show that the normal mode ν_{14} does give rise to $S_{\alpha\alpha}$ terms in the transition tensor. In this case the B_b state is considered to be the main intermediate state since $\langle B_b|\mu_\alpha|G\rangle$ is large. In other words, the transition between the B states and the L_b state becomes dipole allowed. For undisplaced benzene, $\langle L_b|\mu_\alpha|B_b\rangle$ is zero. The Herzberg-Teller expansion of L_b displaced along ν_{14} includes some ground state character giving a non-zero transition dipole moment between the L_b and B_b states. The existence of S_{xx} and S_{yy} transition tensors and a value of zero for the S_{xy}, S_{xz} and S_{yz} transition tensors along with a small (S_{zz} = 1/30S_{xx}) S_{zz} transition tensor does not in and of itself prove the existence of a direct coupling from the L_b to the ground state. Additional calculations done using only the 4 excited configurations give almost identical S_{xx} and S_{yy} values. In this case, the only intermediate states possible are the B states. These states can only induce two-photon activity if the $^1B_{2u}$ state (L_b) is directly coupled to the ground state. So, while other intermediate states may contribute, the net effect of including higher energy states is negligible. Individual states, especially the E_{2g} states, could be mixed into the L_b state. However, the net effect of including them is small. With the orbital coupling discussed previously, it is seen that CNDO and INDO predict the direct coupling of the ground and L_b state for ν_{14} displaced benzene.

Table 10. Transition tensor elements for ν_{14} displaced benzene using MN γ and 196 configurations.

Displacement	S_{xx}	S_{yy}
$0. \times \nu_{14}$	0.	0.
$.25 \times \nu_{14}$	0.02662	0.02653
$.5 \times \nu_{14}$	0.05312	0.05294
$.75 \times \nu_{14}$	0.07935	0.07909
$1. \times \nu_{14}$	0.10520	0.10520

The Born-Oppenheimer breakdown matrix element between the ground and L_b state has been determined in the course of this work by molecular orbital theory. Starting with the matrix element between the ground configuration, $\Phi(G)$ and a singly excited configuration, $\Phi(V^{i\rightarrow m})$ written as,

$$\langle\Phi(G)|\nabla_Q|\Phi(V^{i\rightarrow m})\rangle$$

and noting that

$$\langle\Phi_G| = \langle 1\bar{1}2\bar{2}\ldots p\bar{p}|$$

and

$$|\Phi(V^{i\rightarrow m})\rangle = \frac{1}{\sqrt{2}}(|1\bar{1}2\bar{2}\ldots i\bar{m}\ldots p\bar{p}\rangle - |1\bar{1}2\bar{2}\ldots \bar{i}m\ldots p\bar{p}\rangle),$$

the matrix element between these two configurations with the operator ∇_Q between them is,

$$\langle\Phi(G)|\nabla_Q|\Phi(V^{i\rightarrow m})\rangle = \frac{1}{\sqrt{2}}\Big[(\langle 1\bar{1}2\bar{2}\ldots i\bar{i}\ldots p\bar{p}|(\nabla 1)\bar{1}2\bar{2}\ldots i\bar{m}\ldots p\bar{p}\rangle +$$

$$\langle 1\bar{1}2\bar{2}\ldots i\bar{i}\ldots p\bar{p}|1(\nabla\bar{1})2\bar{2}\ldots i\bar{m}\ldots p\bar{p}\rangle +\ldots+ \langle 1\bar{1}2\bar{2}\ldots i\bar{i}\ldots p\bar{p}|1\bar{1}2\bar{2}\ldots(\nabla i)\bar{m}\ldots p\bar{p}\rangle$$

$$+\ldots) - (\langle 1\bar{1}2\bar{2}\ldots i\bar{i}\ldots p\bar{p}|(\nabla 1)\bar{1}2\bar{2}\ldots\bar{i}m\ldots p\bar{p}\rangle +$$

$$\langle 1\bar{1}2\bar{2}\ldots i\bar{i}\ldots p\bar{p}|1(\nabla\bar{1})2\bar{2}\ldots\bar{i}m\ldots p\bar{p}\rangle +\ldots+$$

$$\langle\bar{1}1\bar{2}2\ldots\bar{i}i\ldots\bar{p}p|1\bar{1}2\bar{2}\ldots(\nabla\bar{i})m\ldots p\bar{p}\rangle +\ldots)\Big].$$

This fearsome looking equation has mostly zeros in it; in fact, the only term that is not zero has the term ∇m. The rest all have the product $\langle i|m\rangle$, which is zero since the orbitals are orthogonal. This makes the matrix element,

$$\langle\Phi(G)|\nabla|\Phi(V^{i\rightarrow m})\rangle = \frac{1}{\sqrt{2}}\langle i|\nabla|m\rangle.$$

In the case of the ground state coupling to the L_b state in benzene, the configurations have been given previously, the BO breakdown electronic matrix element is

$$\langle\Phi(G)|\nabla|\Phi(L_b)\rangle = \frac{1}{\sqrt{2}}(\langle\varphi_{2'}|\nabla|\varphi_3\rangle + \langle\varphi_{3'}|\nabla|\varphi_2\rangle).$$

Recalling that the configurations contribute $2^{-1/2}$ and $-2^{-1/2}$ the matrix element can be calculated by

$$\frac{1}{2}\times\frac{\langle\varphi_{2'}(0)|\varphi_3(Q)-\varphi_3(0)\rangle - \langle\varphi_{3'}(0)|\varphi_2(Q)-\varphi_2(0)\rangle}{Q},$$

where Q is small. If the term $|\varphi(Q) - \varphi(0)\rangle$ is linear with displacement in Q. Here $\varphi(Q)$ represents the molecular orbital at nuclear configuration Q and $\varphi(0)$ is a molecular orbital calculated at the equilibrium geometry. The term $|\varphi_j(Q) - \varphi_j(0)\rangle$ was checked for linearity along normal mode ν_{14}. In all cases deviations from linearity were negligible. Since the orbitals are orthonormal at a given geometry, $\langle\varphi_{2'}(0)|\varphi_3(0)\rangle$ is zero and the BO matrix element is then

$$\frac{\langle\varphi_{2'}(0)|\varphi_3(Q)\rangle - \langle\varphi_{3'}(0)|\varphi_2(Q)\rangle}{Q}.$$

The scalar product $\langle\varphi_i(0)|\varphi_j(Q)\rangle$ was taken by first transforming the orthogonalized molecular orbitals into nonorthogonalized Slater molecular orbitals by using one over the square root of the overlap matrix[78], and taking the displaced molecular orbital and equilibrium geometry molecular orbital and summing the squares of the coefficients over all the atomic centers. For one RMS displacement of ν_{14}, the scalar product for $\langle\varphi_{2'}(0)|\varphi_3(Q)\rangle$ is .0456 and for

$\langle\varphi_3'(0)|\varphi_2(Q)\rangle$ is -.0456, giving a numerator of .0456. Dividing by Q (the carbon displacement for ν_{14}) of .01245 gives an electronic matrix element of 4.5 x 10^{-8} cm^{-1}. The total BO matrix element is

$$\frac{1}{2M/m_e}\langle\varphi|\nabla_Q|\varphi\rangle\langle\chi|\nabla_Q|\chi\rangle,$$

giving a total coupling of 357.9 cm^{-1}. This result shows that the BO breakdown between L_b and the ground state in benzene is on the order of 1/100, the energy gap between these two states.

This correlation between Herzberg-Teller coupling and Born-Oppenheimer breakdown coupling leads to the question, "Are these two forms of state coupling related?" The answer is that they are. Remembering that in the HT expansion, a state Ψ_i is written,

$$|\Psi_i(Q)\rangle = \sum_n c_{ni}|\Psi_n(0)\rangle,$$

and the expansion coefficient c_{ni} is,

$$\langle\psi_n|\nabla_Q H|\psi_i\rangle Q.$$

Taking the derivative with respect to the variable Q in the HT expansion gives,

$$\nabla_k|\Psi_i\rangle = |\Psi_i'\rangle = \sum_n c_{ni}'|\Psi_n(0)\rangle,$$

where the primes indicate differentiation with respect to the coordinate Q. This gives the BO breakdown matrix element between two states Ψ_j and Ψ_i to be,

$$\langle\Psi_j(Q)|\nabla_k|\Psi_i(Q)\rangle = \sum_n\langle\Psi_j(Q)|c_{ni}'|\psi_n(0)\rangle.$$

Then expanding the $\Psi_j(Q)$ in terms of the crude adiabatic basis states, $\psi_m(0)$, gives

$$\sum_m\langle\Psi_m(0)|\nabla_Q|\Psi_i(Q)\rangle = \sum_m c_{mj}c_{mi}'$$

The term $\langle\psi_m(0)|\nabla_Q|\psi_i(Q)\rangle$ is evaluated at Q=0. In the sum on the right-hand side of the equation, the only term that will be nonzero is the term with m=j, since $c_{mj} = \delta_{mj}$. Now, c'_{ji} can be written, assuming the Herzberg-Teller coupling is linear in displacement, as c_{ji}/Q. Thus, there is a direct relationship between the Herzberg-Teller vibronic coupling and Born-Oppenheimer nonadiabatic coupling.

Using the nonadiabatic coupling, time-dependent calculations have been carried out in which an initial wavepacket is propagated between two surfaces. The BO breakdown allows for the possibility of electronic transition between the two potential surfaces without the electric field from light coupling them. This is known as a radiationless transition. The ability to couple two states by the BO breakdown term, or nonadiabatic coupling, was not available in the version of the code obtained from Professor Imre and the program was therefore modified. Testing of this modification was carried out by using two identical harmonic oscillator potentials and starting the wavepacket in the ground state of the lower surface, then comparing the results for the value of the square of the amplitude on each surface with values calculated using a series of harmonic oscillator states. This was chosen since the coupling between two harmonic oscillator states by the momentum operator is exactly known and taking the time dependence of the basis of harmonic oscillator states should give the same results as propagating a wavepacket on a harmonic potential nonadiabatically coupled to an identical surface. The results were identical. These results are shown in Figures 20 and 21. Identical results were also obtained when the wavepacket was started on the upper surface. The results show simple recurrence, just as any simple two-state system coupled by a constant perturbation would.

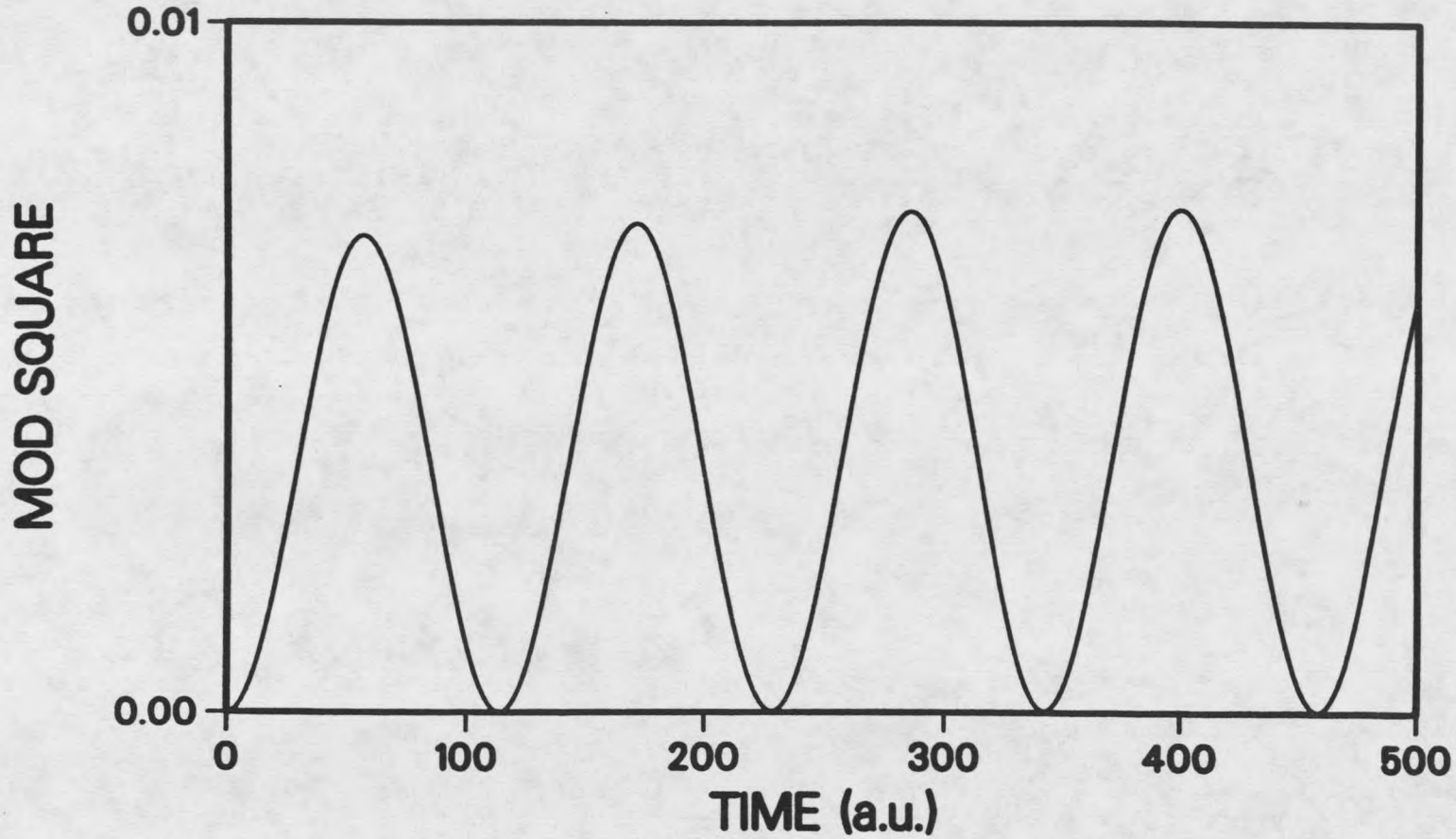

Figure 20. A time dependent calculation using two identical harmonic oscillators and their states obtained by propagating the eigenvalues of the system in time.

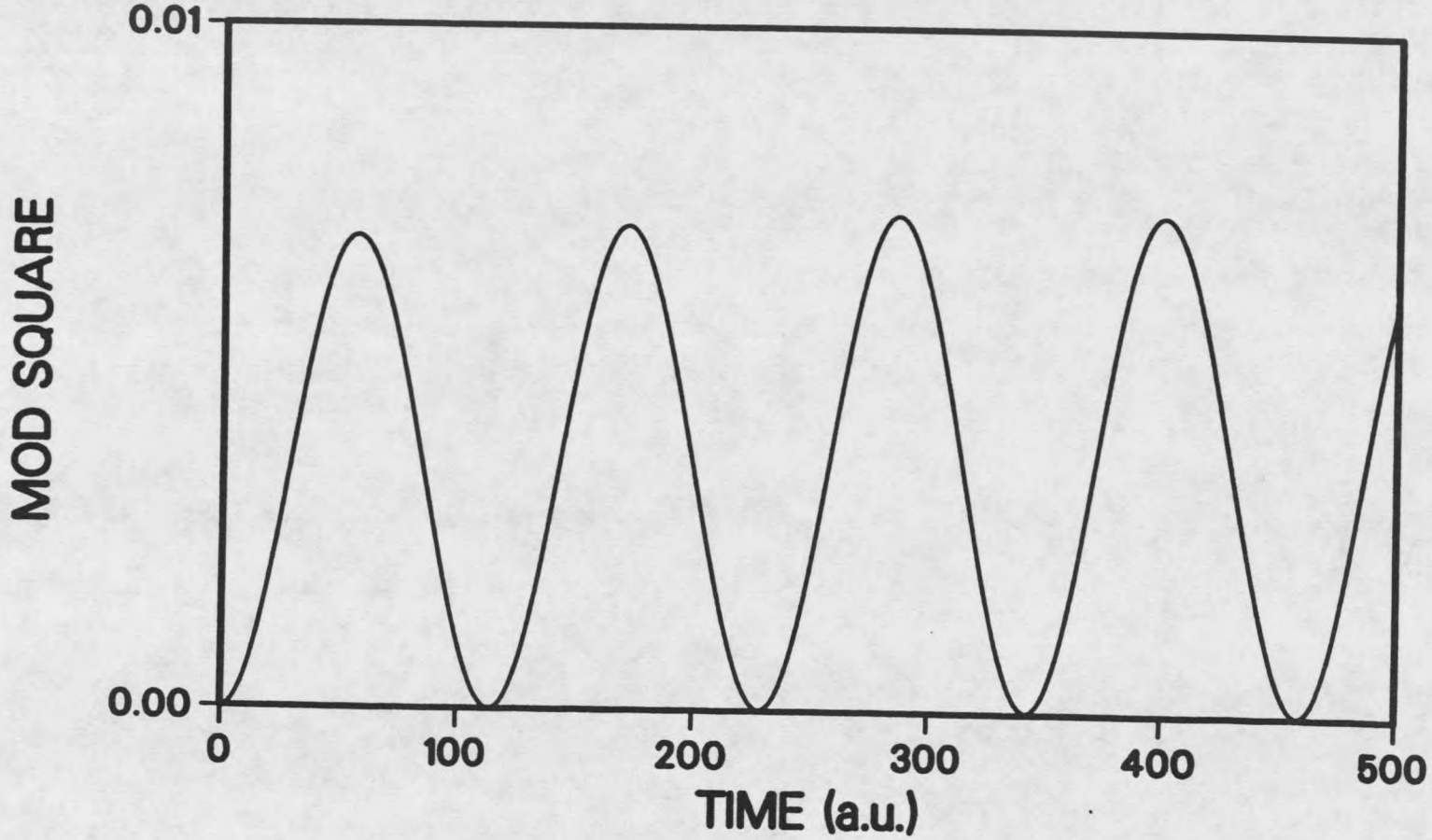

Figure 21. A time dependent calculation using two identical harmonic oscillators and their states obtained by propagating an initial wavepacket along the lower potential.

Having verified the adaptations made after acquisition of the program, the potential was modified to allow for the observed coupling of the two surfaces. These results varied little from the results for identical harmonic oscillator potentials. These calculations have no way for the energy that appears along the lower surface to be absorbed into other motions of the molecule. This model just couples two kinds of molecular energy, the electronic energy and the nuclear energy along the promoting mode. With only two degrees of freedom, it is not unexpected that the system shows recurrence.

Several improvements to the program to model the propagation of the wavepacket in studying radiationless transitions can be made. The first improvement should be to include another degree of freedom on the surfaces. This could be used to include the Franck-Condon active mode ν_1, and possibly provide a way for energy in ν_{14} to "bleed out" of the promoting mode along the ground state surface, possibly preventing the ground state from transferring amplitude to the excited state. Another improvement to the model would be to include possible effects from other excited states.

9-ethylguanine

Table 11 shows the differences in the potential at each atomic center squared and then summed over the entire molecule between a given iteration and the previous iteration to show the convergence of the 9–methylguanine calculations done using the electric field and electrostatic potentials. It is seen that after five to six iterations the potentials do not change very much at all. Several calculations were done using the Slater basis after the iteration eight and the field remained consistent.

Table 11. Sum of differences of the potential squared for the series of calculations using the Slater and Löwdin basis fields.

Iteration	Löwdin Basis	Slater Basis
1	4.016	6.507
2	0.312	0.581
3	0.037	0.072
4	0.028	0.006
5	0.048	0.001
6	0.064	0.130
7	0.002	0.003
8	0.0003	0.0002

Figure 22 and 23 summarize the results of calculations on 9-methylguanine. The panel labeled "No Field" gives the results of oscillator strengths (bar heights) and transition moment directions (direction of arrow at the top of each bar) for the lowest 6 $\pi\pi^*$ transition for the isolated molecule. The panels labeled "Scaled Slater Field" and "Scaled Löwdin Field" give the oscillator strengths and transition moments for the lowest 6 $\pi\pi^*$ transitions, including the electrostatic potentials and the electric field caused by the interaction of the molecule with other molecules in the crystal. These potentials and fields are multiplied by factors of .640 for the Slater field and .718 for the Löwdin field in these two sets of calculations in order to reflect the overestimation of the ground state dipole in INDO/S calculations compared to *Ab initio* calculational results. The panels labeled "Slater Field" and "Löwdin Field" show the results of similiar calculations without the *Ab initio* scaling factor.

The inclusion of the electric fields and electrostatic potentials has a significant effect on transition energies and oscillator strengths. Also, there is a large change in the transition moments. The differences between the results of the calculations seen by the changes in the bars and transition densities in some of the

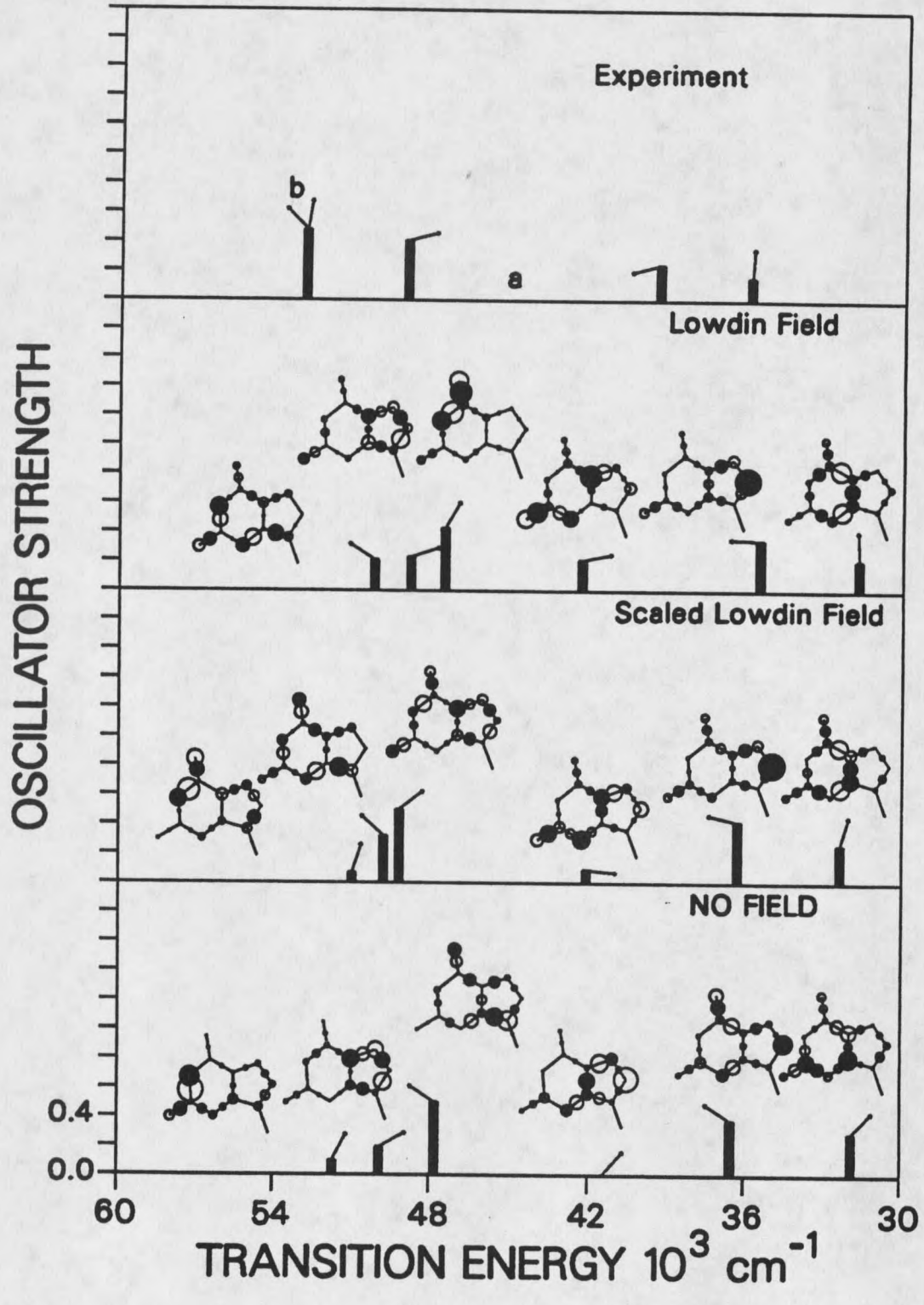

Figure 22. Calculations of 9-methylguanine including the effects of the crystal field calculated in the Löwdin basis.

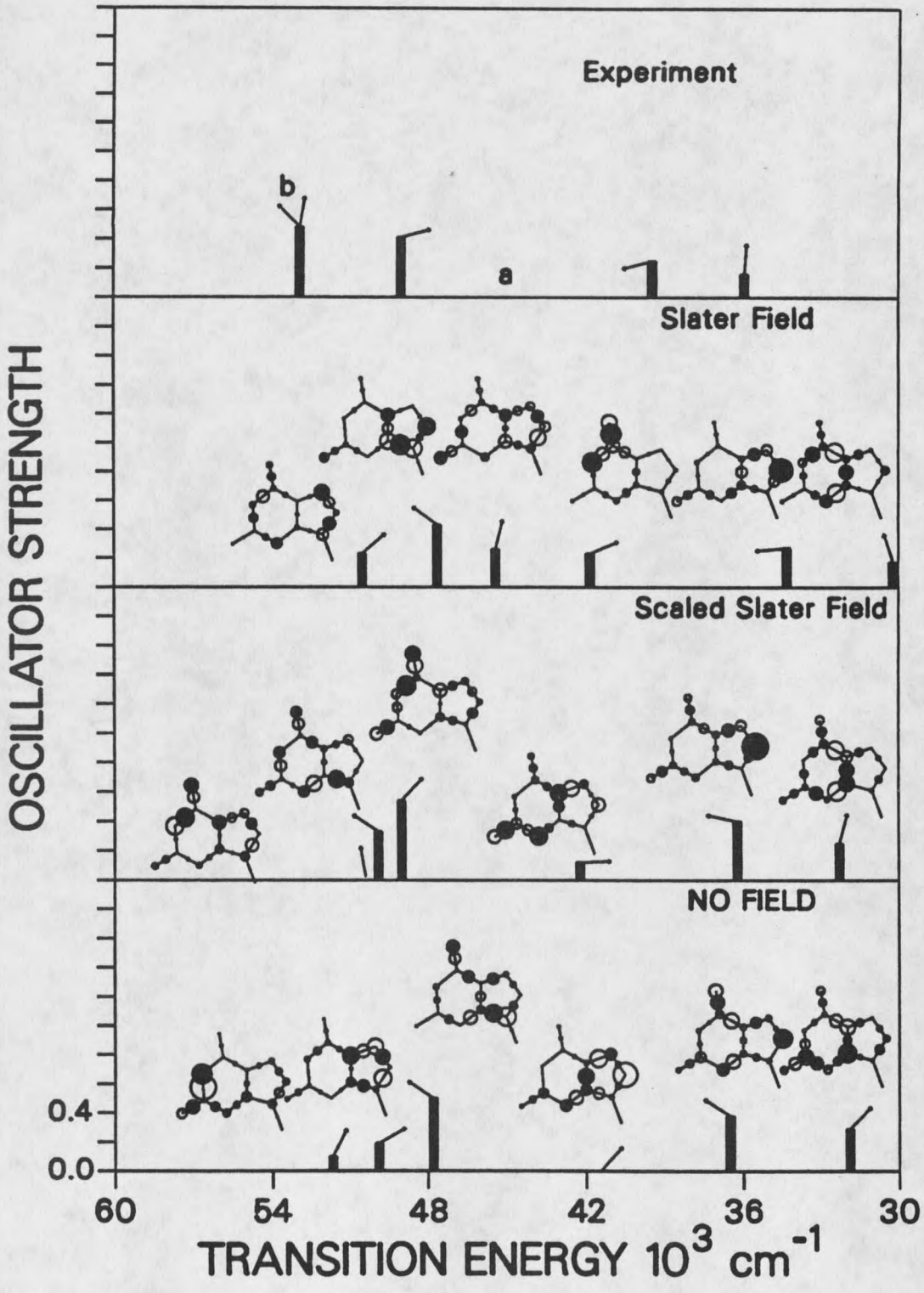

Figure 23. Calculations of 9-methylguanine including the effects of the crystal field calculated in the Slater basis.

panels, is due to the large mixing that occurs between $\pi\pi^*$ states and also some mixing with $n\pi^*$ states. These changes are a result of significant molecular orbital mixing and reordering of molecular orbital energies. These orbitals lead to changes in the transition character since transitions between molecular orbitals make up the excited states. The molecular orbitals pictured in Figures 24-27 show how the crystal field changes the shape of the orbitals. It also reveals that in using the scaled Löwdin field based on orthogonalized orbitals gives only minor differences compared to the scaled Slater field, which is based on nonorthogonalized orbitals. In terms of the lowest $\pi\pi^*$ states the orbital effect of most importance is the effect on the LUMO, LUMO+1 and LUMO+2, orbitals 32, 33 and 34. The LUMO and LUMO+1 orbitals are inverted in relative energy. The orbital changes over all the occupied molecular orbitals show the net result of the field is to move electron density towards the carbonyl oxygen and N_7. This result is expected, since these atoms are donating electrons through hydrogen bonds to protons on other molecules in the crystal. It is then expected that the relative energies of their atomic orbitals will be lowered. The lowest $\pi\pi^*$ transition in 9–methylguanine is largely a HOMO $\rightarrow$ LUMO transition, that is the configuration interaction coefficient for that configuration is by far the largest in making up this state. The second $\pi\pi^*$ state is largely a HOMO $\rightarrow$ LUMO+1 transition and so the reversal of the LUMO and LUMO+1 orbitals will result in different properties for the lowest $\pi\pi^*$ and the second $\pi\pi^*$ state from the unperturbed molecule.

In Figure 28 the electrostatic potential is shown using the values for the final iteration with the scaled Löwdin field with positive potentials represented by open circles and negative potentials represented by filled circles. The potentials

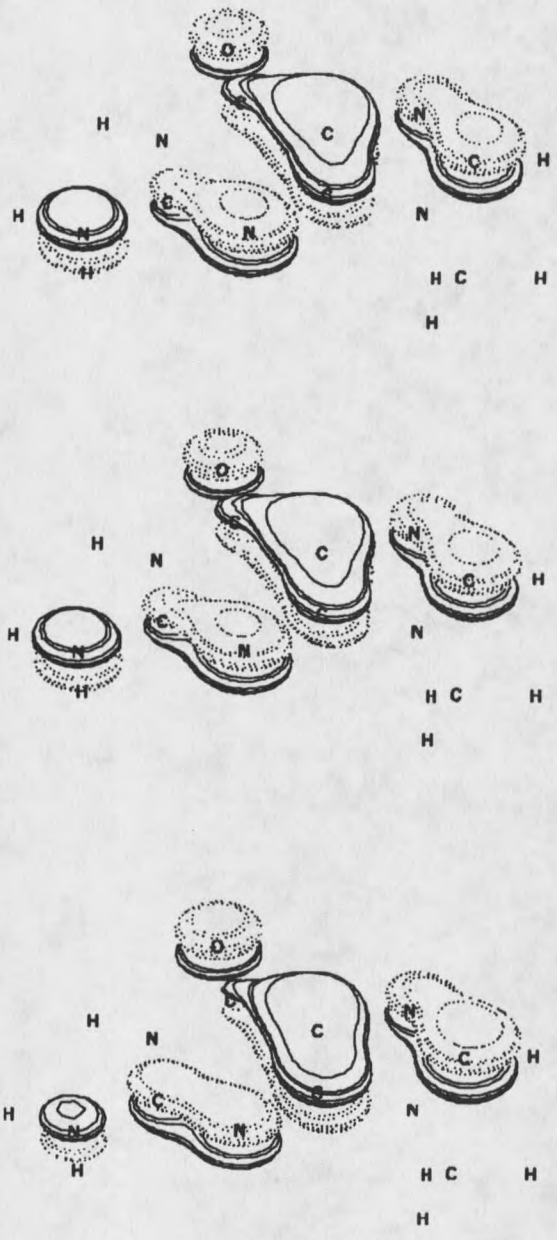

Figure 24. The HOMO (MO 31) of 9-methylguanine calculated with no field (bottom), with the scaled Löwdin field (middle) and with the scaled Slater field (top)

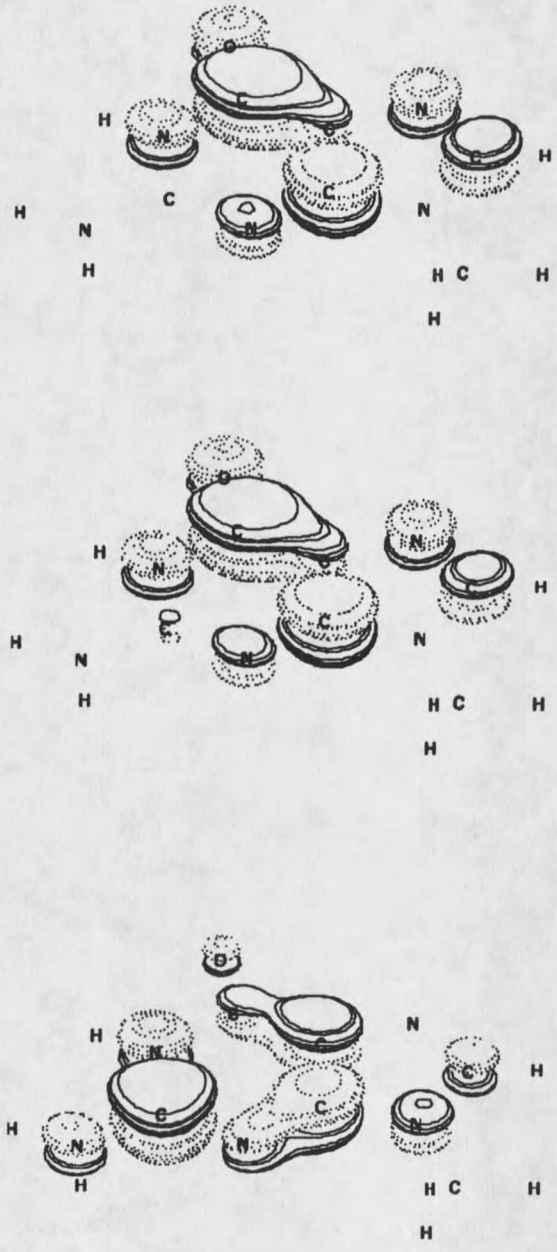

Figure 25. The LUMO (MO 32) of 9-methylguanine calculated with no field (bottom), with the scaled Löwdin field (middle) and with the scaled Slater field (top)

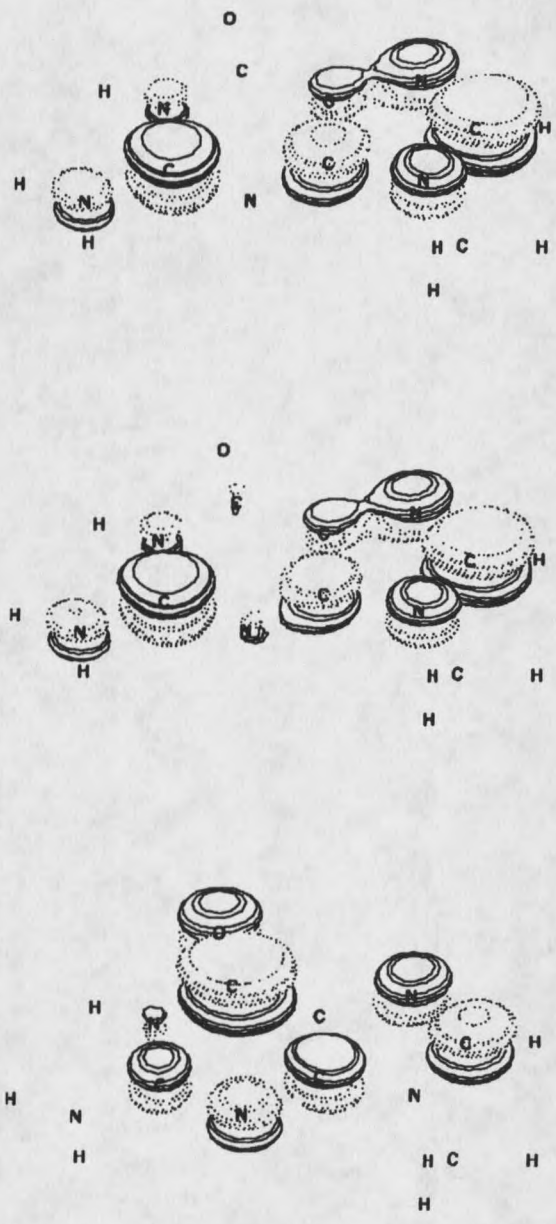

Figure 26. The LUMO+1 (MO 33) of 9-methylguanine calculated with no field (bottom), with the scaled Löwdin field (middle) and with the scaled Slater field (top)

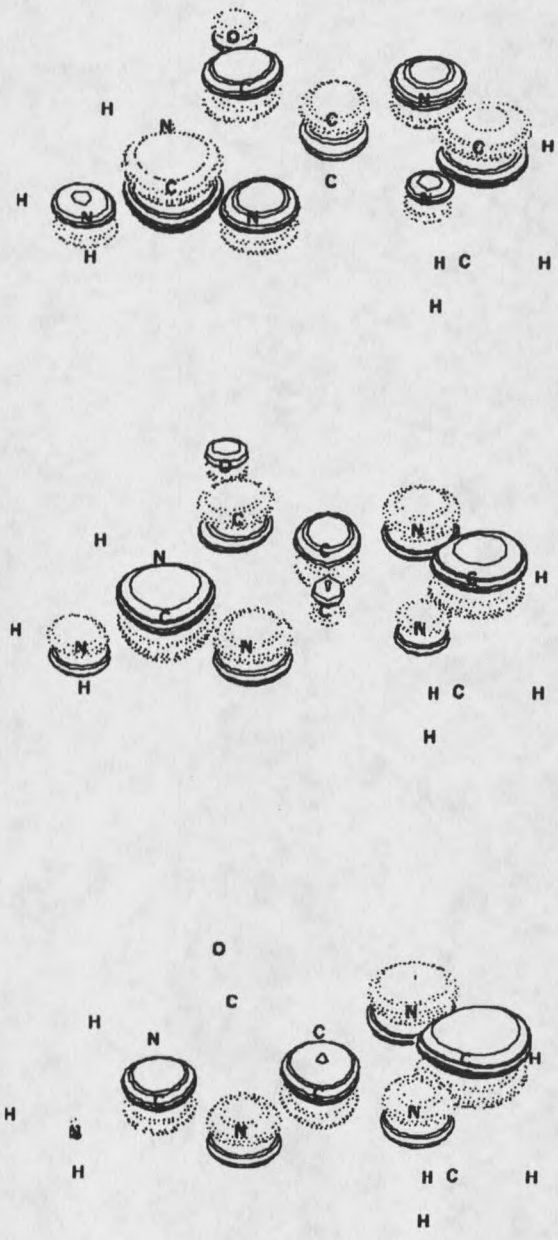

Figure 27. The LUMO+2 (MO 34) of 9-methylguanine calculated with no field (bottom), with the scaled Löwdin field (middle) and with the scaled Slater field (top)

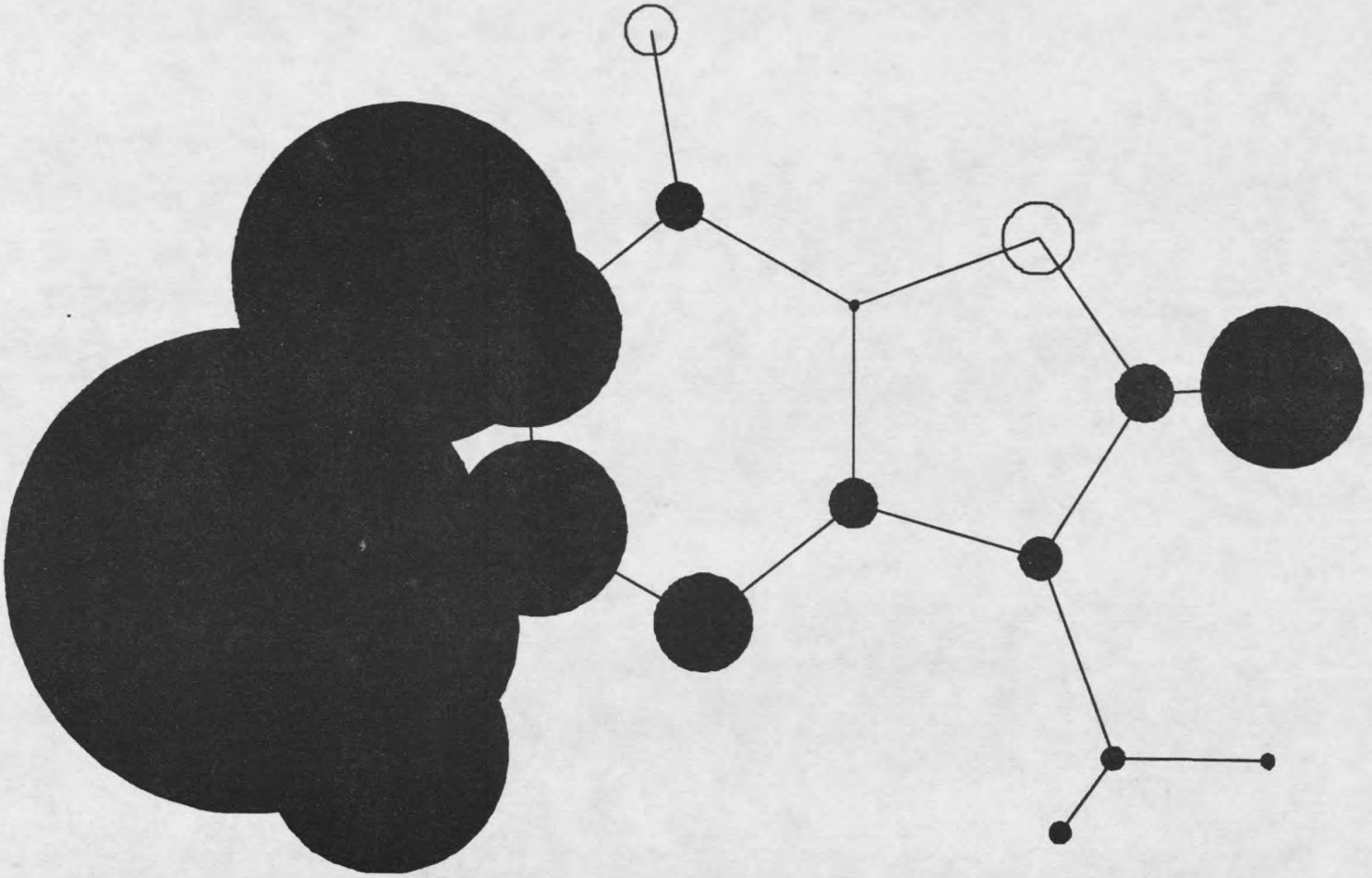

Figure 28. The potential at each atomic center due to the crystal field in 9-methylguanine.

and electric field components are also shown in Table 12. It should be pointed out here that a positive electrostatic potential at a given atomic center will result in a lowering of the diagonal Fock matrix element associated with that center.

Table 12. The electric field vectors along with the electrostatic potentials using the final iteration of the scaled Löwdin field.

Atomic Center	Electric Field e_x	e_y	e_z	Electrostatic Potential
N_1	-0.010629	0.287041	-0.047415	-0.445389
C_2	0.016371	0.210224	0.010030	-0.405493
N_3	-0.030262	0.124478	0.076650	-0.224579
C_4	-0.018647	0.059038	-0.004724	-0.112205
C_5	-0.138949	0.103047	-0.081559	-0.019529
C_6	-0.166226	0.205194	-0.103714	-0.105116
N_7	-0.333159	-0.003087	-0.044536	0.166288
C_8	-0.080274	-0.160593	-0.026787	-0.131059
N_9	0.014557	-0.026922	-0.012560	-0.095969
N_{10}	0.074301	0.315147	0.028234	-0.671255
O_{11}	-0.243345	0.277118	-0.072088	0.116344
H_{12}	0.109208	0.200768	0.080158	-0.571461
H_{13}	0.102420	0.693542	0.090479	-1.120734
H_{14}	0.174984	0.583092	0.073062	-0.800299
H_{15}	0.039050	-0.357533	0.057849	-0.375975
C_{16}	0.036842	0.011846	0.012258	-0.051126
H_{17}	0.069080	0.047685	-0.029872	-0.029466
H_{18}	0.024159	0.042380	-0.012428	-0.047376
H_{19}	-0.012398	0.017074	0.078621	-0.006734

The energy shifts for all the π molecular orbitals are pictured in Figure 29 using the scaled Löwdin field. Table 13 gives the values for the molecular orbital energies calculated without the crystal field present, the first order energy correction e^{ii}:F′, calculated using the scaled Löwdin field and the orbital energies calculated with the same field present by INDO/S. The field shifts orbital energies of the LUMO and LUMO+1 by .0478 a.u. and .0259 a.u. in first order respectively. The shift in the LUMO energy is large and positive reflecting the destabilization of this orbital, not unexpected since the LUMO has a large

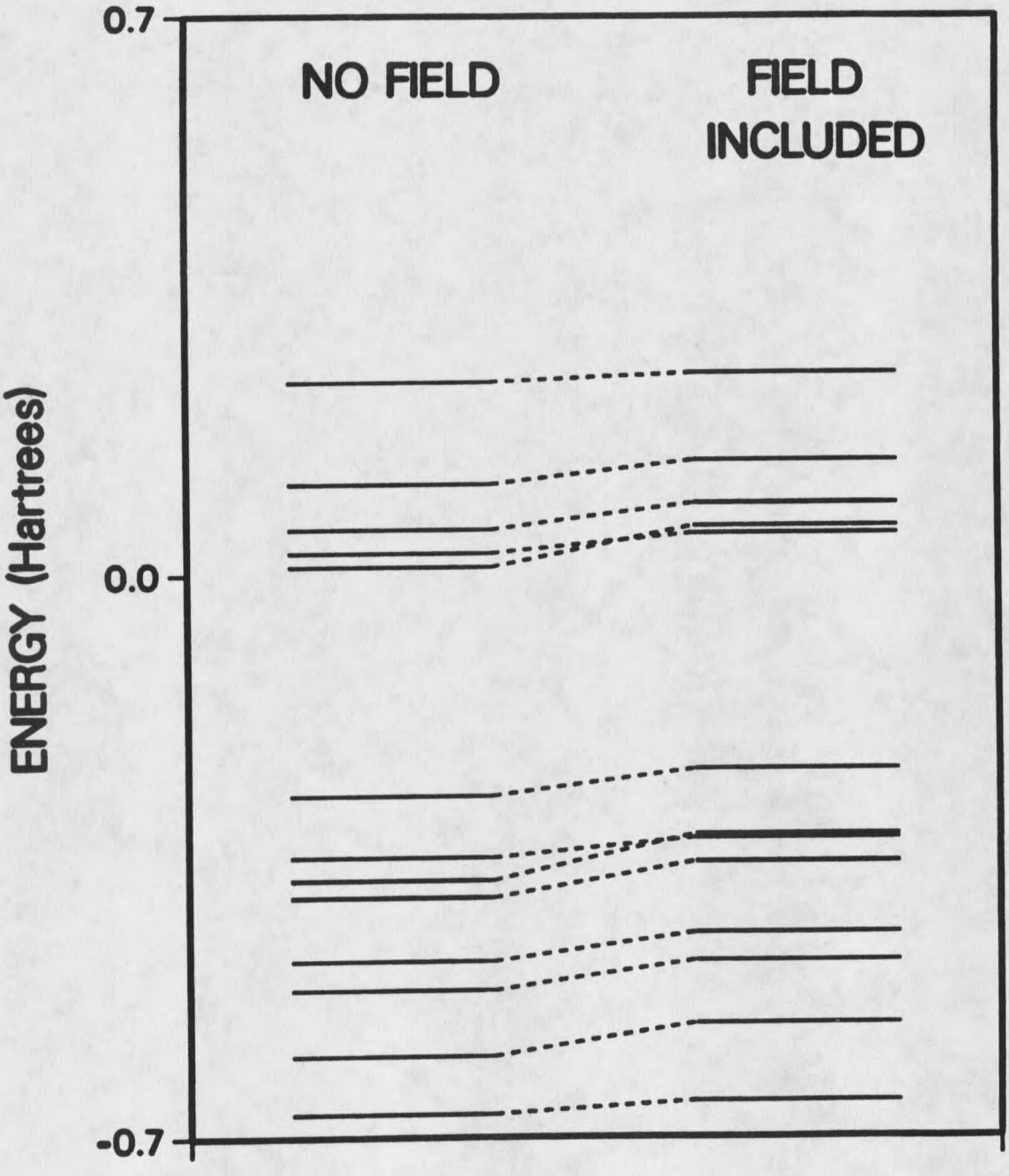

Figure 29. Orbital energy changes caused by the scaled Löwdin electric field and potentials.

contribution from the π atomic orbitals on N_1, C_2, N_3 and N_9. These centers become less favorable sites for electron density in the presence of the field. For the LUMO+1 the change is not as large since this orbital has a large contribution from the π atomic orbitals on C_6 and O_{10}. Electron density on these centers is stabilized by H bonding to a neighboring molecule in the crystal. Again, in this case the change in the Fock matrix gives a good characterization of the perturbation on the molecule as predicted by CNDO/S through the mapping of the Fock matrix directly onto the transition density matrix.

Table 13. Energies of selected π molecular orbitals and their first order changes.

Molecular orbital	Energy (No Field)	Scaled Löwdin Field $F':\rho^{i,i}$	Energy Field On
31	−0.2766	0.0321	−0.2444
32	+0.0089	0.0478	+0.0497
33	+0.0262	0.0259	+0.0587
34	+0.0552	0.0265	+0.0867

The Fock matrix mapped onto the density of an individual orbital gives reasonable agreement with the INDO/S calculated energies. To determine if the expression $F':\rho^{KL}$ is a good approximation for the interaction between two states in the effect of crystal field interactions in the 9-ethylguanine calculations, an analysis was carried out using the states calculated by INDO/S without the field as a basis set. This analysis is similar to calculations carried out by Woody.[38] The first order correction of the first two $\pi\pi^*$ basis states is $F':\rho^{KK}$ and the interaction between these two states is $F':\rho^{KL}$. The values for the first order changes and the interaction for these two states are 8.00×10^{-3} a.u., 3.94×10^{-5} a.u. and -1.06×10^{-2} a.u. respectively. Adding the first order corrections to the state energies calculated without the field gives an energy difference between the states of 2.8×10^{3} cm^{-1}.

Setting up a 2×2 determinant using the states with the first order energy correction and the interaction gives

$$\begin{vmatrix} 33.7 & -2.2 \\ -2.2 & 36.5 \end{vmatrix}.$$

Solving the equations gives,

$$\Psi_1(F) = .8766\Psi_1(0) + .4812\Psi_2(0),$$

where $\Psi(F)$ represents the state with the field and $\Psi(0)$ represents the state without the field.

The states in the presence of the field can be transformed through the configurations that make up the states, so the INDO/S calculations can be made to yield the perturbed states as a linear combination of the basis states. In this language the perturbed states are the states with the field present and the basis states are the states calculated without the field. Transforming the perturbed states gives

$$\Psi_1(F) = .8682\Psi_1(0) + .4005\Psi_2(0) - .1272\Psi_3(0)$$

for the lowest excited $\pi\pi^*$ state and

$$\Psi_2(F) = -.3057\Psi_1(0) + .8079\Psi_2(0) - .4361\Psi_3(0)$$

for the second $\pi\pi^*$ state.

The expression $F':\rho^{KL}$ is shown here to give an accurate representation of the interaction caused by the crystal field between the lowest $\pi\pi^*$ states in guanine just as the same expression did in the case of vibronic coupling of the benzene $^1B_{2u}$ state to the $^1E_{1u}$ state. Again, in this case, the change in the Fock matrix mapped directly onto the transition density matrix between the states gives a good characterization of how the perturbation of the molecule will mix the states in a CNDO/S or INDO/S calculation. The effect of the crystal field on the molecule is about ten times the relative changes in the Fock matrix elements caused by

vibrations in benzene. The large fields are due to the crystal structure itself and to the size of the monopoles on the hydrogens, oxygen and nitrogens involved in the hydrogen bonding in the crystal. The charge distribution is shown in Table 14 and Figure 30 as the formal charges associated with each atomic center. Figure 31 shows the hydrogen bonding pattern that is present in the crystal structure.[79] The carbonyl oxygen and N_9 are in close proximity to hydrogens attached to N_1 and N_{10}. This picture is consistent with the field effects seen in the calculations, that the hydrogen bonds stabilize electron density on the oxygen and N_9.

Table 14. Formal charges associated with each atomic center in 9-methylguanine calculated with no external field

Atomic Center	Löwdin Basis	Slater Basis
N_1	-0.119	-0.319
C_2	0.350	0.485
N_3	-0.404	-0.476
C_4	0.180	0.258
C_5	0.018	0.095
C_6	0.396	0.512
N_7	-0.316	-0.394
C_8	0.144	0.191
N_9	-0.070	-0.237
N_{10}	-0.231	-0.455
O_{11}	-0.608	-0.683
H_{12}	0.152	0.254
H_{13}	0.149	0.216
H_{14}	0.158	0.247
H_{15}	0.064	0.127
C_{16}	0.058	-0.009
H_{17}	0.023	0.058
H_{18}	0.028	0.065
H_{19}	0.028	0.065

Figure 32 displays the transition density between the two lowest $\pi\pi^*$ states in 9-methylguanine along with the transition densities for the lowest two $\pi\pi^*$ states calculated without the crystal field. It can be seen that the phase of the transition

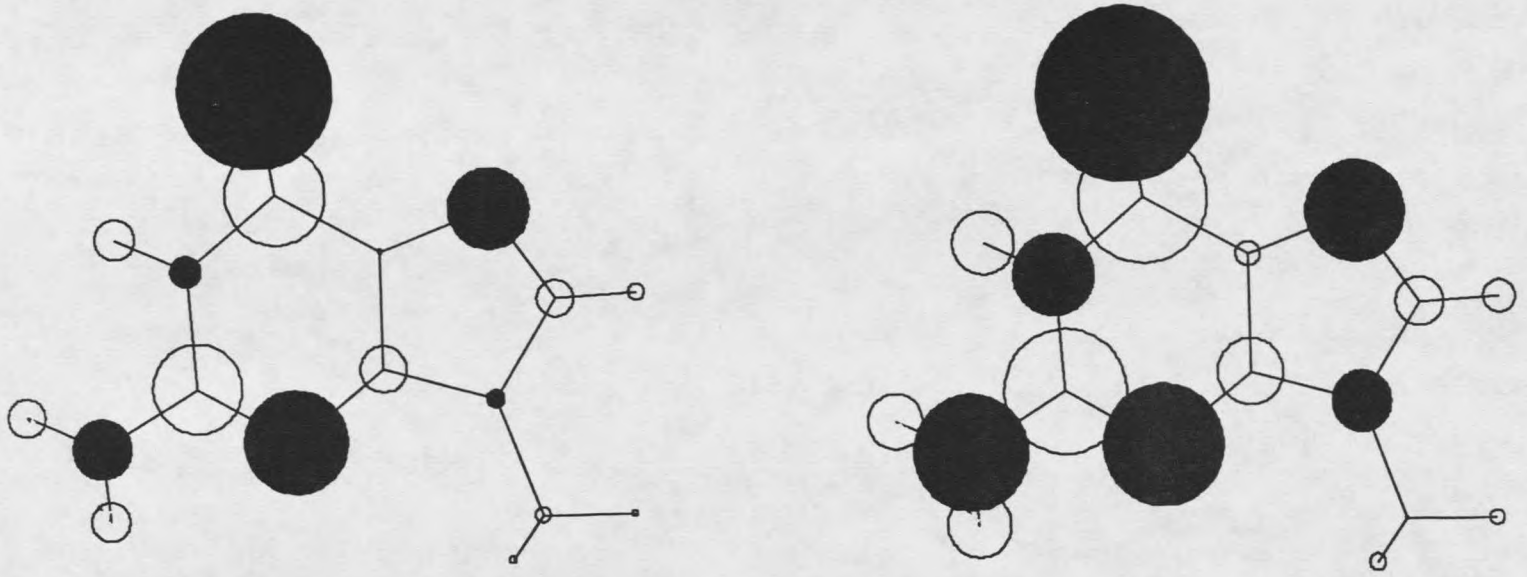

Figure 30. Formal charges for 9-methylguanine calculated in the Löwdin basis (left) and the Slater basis (right).

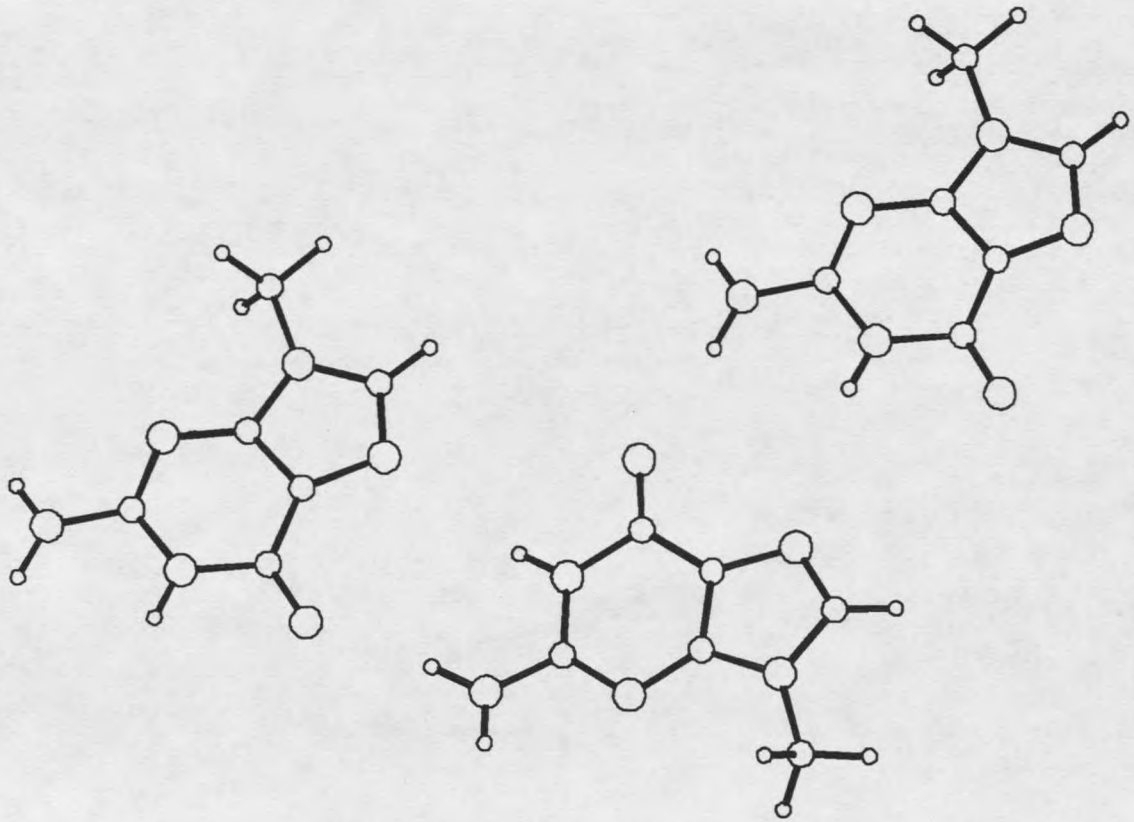

Figure 31. 9-methylguanine with neighboring molecules and the hydrogen bonding pattern in the crystal.

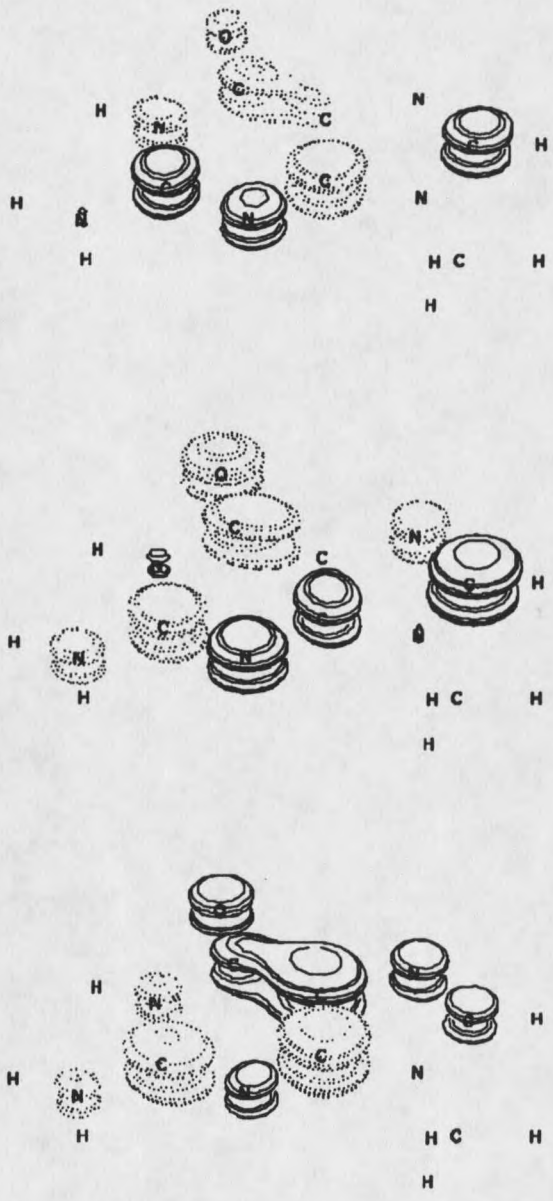

Figure 32. The transition density between the first two $\pi\pi^*$ states in 9–methylguanine (top), the transition density between the ground state and the second $\pi\pi^*$ state (middle) and the transition density between the ground state and the lowest $\pi\pi^*$ state.

density is opposite that of the change in the Fock matrix due to the crystal field, the dotted contours in the transition density overlap with the solid contours in the Fock matrix change. This leads to the negative sign in the off-diagonal matrix element between the two states and rotates the calculated transition moment directions toward the experimental values rather than away from them.

From these calculations it is seen that INDO/S calculations can accurately reflect the transition moments of the lowest two $\pi\pi^*$ states in 9-ethylguanine when the effect of neighboring molecules in the crystal are included. Furthermore, the observed transition moments from the single crystal absorbance measurements is not the same as in the isolated molecule, since the field caused by the presence of the crystal is so large. It is also possible that solvation effects on molecules with such large dipole moments can significantly mix orbitals and therefore states. Currently, calculations are being carried out using the same method described here on other DNA bases.

CONCLUSIONS

In this work the equation $H'_{ij} = F':\rho^{ij}$, using a basis of molecular orbitals that polarize as well as float along with the nuclei as they move, has been used to approximate the mixing of two electronic states. This equation has proven useful in the three cases studied here. The question of generality will be addressed here.

We start by considering two states Ψ_K and Ψ_L, where

$$\Psi_K = \sum_\kappa d_{K\kappa}\chi_\kappa$$

$$\Psi_L = \sum_\lambda d_{L\lambda}\chi_\lambda,$$

and χ is a singly excited configuration in which an electron is removed from orbital i and placed in orbital k. The matrix element between two states is, neglecting again the change in the ds,

$$\begin{aligned} H'_{KL} = \sum_{\kappa,\lambda} [&F':(\rho^{kk} + \rho^{ll} - \rho^{ii} - \rho^{jj} + \rho^{kl}\delta_{ij} - \rho^{ij}\delta_{kl}) + \\ &F:(\rho^{kk} + \rho^{ll} - \rho^{ii} - \rho^{jj} + \rho^{kl}\delta_{ij} - \rho^{ij}\delta_{kl})' + \\ &\gamma':(2\rho^{ik,jl} - \rho^{ij,kl}) + \gamma:(2\rho^{ik,jl} - \rho^{ij,kl})']\ (d_K d_L). \end{aligned}$$

In the parentheses of the first two terms is the quantity ρ^{KL}, the transition density between state K and L. Combining the first two terms and calling them F′ and the last two terms into a term called R′, the equation can be rewritten,

$$H' = F' + R'.$$

Consider now an imaginary molecule with only four molecular orbitals, two of which are occupied. The occupied orbitals, i and j, along with the two virtual orbitals, k and l, can give rise to four singly excited configurations, χ_i^k, χ_i^l, χ_j^k,

and χ_j^l. The mixing of states arising from these configurations can be classified by the relative sizes of the terms F′ and R′.

There are two possibilities here:

Case 1). $F' >> R'$

Now the state mixing is governed by the equation

$$H' = F' = F':(\rho^{LK})^\circ + F^\circ:(\rho^{LK})'.$$

There are two subcases here:

Case 1a) $F':(\rho^{LK})^\circ >> F^\circ:(\rho^{LK})'$

This is the case into which the three systems that have been discussed here fall.

It is necessary for the two states to have one of two things; 1). Common configurations, that is, two states must share configuration χ_i^k, or 2). Separate configurations which have a common molecular orbital, that is, if one state contains configuration χ_i^k, the other state must contain either configuration χ_i^l or χ_j^k.

If the states contain the same configurations, then the mixing is expressed in changes to the configuration interaction matrix. In benzene, the $^1B_{2u}$ state L_b no longer has equal contributions from the two configurations that make up the zeroth order state.

If the states are made up of configurations which share one, and only one, orbital, then the changes in the states are brought about by the mixing, or polarization, of the molecular orbitals that are not held in common. In other words, the important change is in the mixing of molecular orbitals k and l if the states each contain configurations that have molecular orbital i in them.

Case 1b) $F':(\rho^{LK})^\circ$ does not dominate

This case is a second order effect and restricted to configurations that share one molecular orbital. Here, the effect of molecular orbital mixing must be large and

map onto the Fock matrix while the change in the Fock matrix must either be small or not map well onto the transition bond order. The chance of these two events occurring at the same time is unlikely with one exception, when the two orbitals not held in common happen to be degenerate either by group theory or because of accidental degeneracy. If it happens, for example, that orbitals k and l are degenerate then a small interaction could lead to a large mixing of the degenerate orbitals.

Case 2) $F' \approx 0$

This case is totally restricted to vibronic effects, since inclusion of crystal field or solvent effects will not change the Coulomb matrix at all. States that have no common configurations or configurations with common molecular orbitals will fall into this case. The small changes that occur in the Coulomb matrix will generally make this contribution small. Stretching modes such as ν_8 and ν_{14} in benzene will allow, if the transition bond order is nonzero in the near-neighbor positions, this term to be significant. In this study, however, the change in the Fock matrix has been much larger and these situations then fall into Case 1a with a small correction due to the R'_{KL} term.

SUMMARY

For the $B_{2u}(L_b)$ state of benzene, this work has shown that the ratio of the induced oscillator strength, for the e_{2g} normal modes ν_6 and ν_8, or f_6:f_8, is less sensitive to the actual normal mode displacements than to the nature of the electron repulsion scheme (γ) that is used. The ν_8 intensity can be made to vanish by a number of mode/parameter combinations. It has been shown for the first time that in the case of the weak vibronic coupling between the L_b and the allowed B_b state explicit electrostatic terms resulting from charge migration associated with changes in bond angles and lengths play a critical role. The shifting of orbital energies as is reflected by the equation $\Delta E = \rho^{ii}:F'$ determines the strength of the intensity induced through vibronic coupling. This expression for the energy change leads to a prediction for the coupling of two electronic states in the CNDO calculations, given by $H'_{KL} = F':\rho^{KL}$, where ρ^{KL} is the transition density between two electronic states. This is a simple matrix operation where the corresponding elements of the two matrices are multiplied and then the sum is taken over the entire resulting matrix. In the case of the benzene L_b one photon intensity, the two states of importance are the L_b state and the dipole allowed B_b state. In the second excited state of benzene, $B_{2u}(L_a)$ the changes in the exact form of the normal modes is what determines the induced vibronic coupling intensity. Calculations using recent determinations of the normal modes for ν_6 and ν_9 show, for the first time and in agreement with experiment, that ν_9 is more effective in inducing intensity into the L_a state than ν_6.

In the vibronic coupling of the b_{2u} mode ν_{14} the electronic changes are on the off-diagonal positions. The term $F':\rho^{Lb,G}$ in this case predicts direct coupling of the L_b state to the ground state. This result implicates the mode ν_{14} as a suspect in the "Channel Three" mystery, the rapid increase in the nonradiative decay rate of the benzene L_b state when the excitation energy increases over 3000 cm^{-1} above the L_b threshold. The direct coupling to the ground state caused by ν_{14} could lead to direct internal conversion, causing rapid nonradiative decay.

Another case where electrostatic interactions are important is in the crystal field effects of 9-ethylguanine. The electric field and electrostatic potential due to neighboring molecules in the 9-ethylguanine crystal is shown to affect orbital energies and the character of the electronic states. The orbital energy shifts are large enough that the lowest unoccupied molecular orbital (LUMO) and the next molecular orbital higher in energy (LUMO+1) switch positions and mix to give results that are in agreement with experiment. The effect of the field on the molecule is large -- so large that the interaction of the first two $\pi\pi^*$ states is on the order of the energy separation between the two states. In this case also, $F':\rho^{KL}$ predicts the coupling of the electronic states caused by the perturbation and is useful in predicting the mixing of the lowest two $\pi\pi^*$ states. The apparent failure of semiempirical calculations in predicting the transition moment directions of the states is due to the fact that these calculations are done on an isolated molecule. Crystal field effects have not been included prior to this work. A significant result from this work is the implication that the transition moment directions for guanine are sensitive to environment and may be very different in DNA itself than they are in the crystal.

The equation $H'_{KL} = \mathbb{F}':\rho^{KL}$, based on the floating polarizable basis set, used to calculate the perturbation matrix elements has been demonstrated to give good agreement with directly calculated CNDO/S results in the three cases studied.

The success of this method is encouraging and it would be of interest to apply this perturbation formula to other "failures" of the semiempirical methods, such as the fluorobenzene[80] problem and the question of why the 2 position is more sensitive to inductive perturbation than the 1 position in naphthalene.[81]

REFERENCES

1. J.H. Calloman, T.M. Dunn and I.M. Mills, Phil. Tran. Roy. Soc. (London) A259, 499 (1966); G. Fischer, Chem. Phys. Lett. 56, 186 (1978).
2. L. Zeigler and A.C. Albrecht, J. Chem. Phys., 60, 3558 (1974).
3. F. Metz, M.J. Robey, E.W. Schlag and F. Dorr, Chem. Phys. Lett., 51, 8 (1977).
4. T.A. Stephenson, P.L. Radloff and S.A. Rice, J. Chem. Phys. 81, 1060 (1984).
5. D.J. Muller and A.E.W. Knight, J. Phys. Chem., 88, 3392 (1984).
6. W. Hug and I. Tinoco, J. Am. Chem. Soc., 95, 2803 (1973).
7. P.R. Callis, Photochem. and Photobio., 44, 315 (1986).
8. L.B. Clark, J. Am. Chem. Soc., 99, 3934 (1977).
9. D.M. Friedrich and W.M. McClain, Chem. Phys. Lett., 32, 541 (1975).
10. F. Metz, Chem. Phys. Lett., 34, 109, (1975).
11. E. Clar, *Aromatiche Kohlenwasserstoffe*, (Julius Springer, Berlin) (1941).
12. M.G. Mayer and A.L. Sklar, J. Chem. Phys., 6, 645 (1938).
13. C.C.J. Roothaan and R.S. Mulliken, J. Chem. Phys., 16, 118 (1948).
14. A.L. Sklar, J. Chem. Phys., 10, 135 (1942).
15. J.R. Platt, J. Chem. Phys., 17, 484 (1949).
16. E. Hückel, Zeits. F. Physik, 70, 204 (1931).
17. J.E. Lennard-Jones, Proc. Roy. Soc., 158A, 280 (1937).
18. W. Moffitt, J. Chem. Phys., 22, 320 (1954).
19. A.D. McLachlan, Mol. Phys., 2, 271 (1959).
20. W.E. Donath, J. Chem. Phys., 41, 626 (1964).
21. R. Pariser, J. Chem. Phys., 24, 250 (1956).

22. P.R. Callis, T.W. Scott and A.C. Albrecht, J. Chem. Phys., 78, 16 (1983).

23. R. McWeeny, Proc. R. Soc. London Ser. A, 253, 242 (1959).

24. M. Born and R. Oppenheimer, Ann. Phys., 84, 457 (1927).

25. M. Born and K. Huang, *Dynamical Theory of Crystal Lattices*, (Oxford Univ. Press, London), 402-405 (1962).

26. G. Fischer, *Vibronic Coupling*, (Academic Press, London), 35 (1984).

27. G. Herzberg and E. Teller, Z. Phys. Chem. Abt. B, 21, 410 (1933).

28. A. Liehr, Z. Naturforsch., 13a, 311 (1958).

29. R.G. Parr, *Quantum Theory of Molecular Electronic Structure*, (Benjamin, New York) (1963).

30. J.A. Pople and D.L. Beveridge, *Approximate Molecular Orbital Theory*, (McGraw-Hill, New York) (1970).

31. J.A. Pople, D.P. Santry and G.A. Segal, J. Chem. Phys., 435, 129 (1965).

32. J.A. Pople and G.A. Segal, J. Chem. Phys., 43, S136 (1966); J. Chem. Phys., 44, 3289 (1966).

33. J.A. Pople, D.L. Beveridge and P.A. Debosh, J. Chem. Phys., 47, 2026 (1967).

34. J. Del Bene and H.H. Jaffé, J. Chem. Phys., 48, 1807 (1968); 48, 4050 (1968).

35. J. Ridley and M. Zerner, Theoret. Chim. Acta (Berl.), 32, 111 (1973).

36. H. DeVoe and I. Tinoco Jr., J. Mol. Biol., 4, 500 (1962).

37. B. Pullman and A. Pullman, Mol. Biol., 9, 327-402 (1969).

38. R.W. Woody, Biophys. J., 45, 232 (1984).

39. G. Fischer, *Vibronic Coupling*, (Academic Press, London), 93 (1984).

40. D. Kosloff and R. Kosloff, J. Comp. Phys., 52, 35 (1983).

41. R. Kosloff, J. Phys. Chem., 92, 2087 (1988).

42. R. Kosloff and D. Kosloff, J. Chem. Phys., 79, 1823 (1983).

43. S.Y. Lee and E.J. Heller, J. Chem. Phys., 71, 4777 (1979).

44. S.O. Williams and D.G. Imre, J. Phys. Chem., 92, 3363 (1988).

45. K. Krogh-Jespersen, R.P. Rava and L. Goodman, J. Phys. Chem., 88, 5503 (1984).

46. A.G. Ozkabak, L. Goodman, S.N. Thakur and K. Krogh-Jespersen, J. Chem. Phys., 83, 6047 (1985).

47. A.C. Albrecht, J. Chem. Phys., 33, 156 (1960).

48. A.C. Albrecht, J. Chem. Phys., 33, 169 (1960).

49. M.J. Robey and E.W. Schlag, J. Chem. Phys., 67, 2775 (1977).

50. J.N. Murrell and L. Salem, J. Chem. Phys., 34, (1961) 1914.

51. M. Roche and H.H. Jaffé, J. Chem. Phys., 60 1193 (1974).

52. W.C. Johnson Jr., and O.E. Weigang Jr., J. Chem. Phys., 63 2135 (1975).

53. B. Hudson, Private Communication.

54. D.H. Whiffen, Phil. Trans. R. Soc. (London), A248 131 (1955)

55. A.C. Albrecht, J. Mol. Spectrosc., 5, 236 (1960).

56. H. Guo and M. Karplus, J. Chem. Phys., 89 (1988) 4253.

57. P.R. Callis, Intern. J. Quantum Chem., 518, 579 (1984).

58. L. Wunsch, H.J. Neusser and E.W. Schlag, Chem. Phys. Lett., 32, 210 (1975).

59. N. Mikami and M. Ito, J. Chem. Phys., 64, 3077 (1976).

60. J.H. Callomon, J.E. Parkin and R. Lopez-Delgado, Chem. Phys. Lett., 13, 125 (1972).

61. E. Riedle, J.H. Neusser and E.W. Schlag, J. Phys. Chem., 86, 4847 (1982).

62. E. Riedle and H.J. Neusser, J. Chem. Phys., 80, 4686 (1984).

63. U. Schuber, E. Riedle, H.J. Neusser and E.W. Schlag, J. Chem. Phys., 84, 6182 (1986).

64. H.J. Neusser, U. Schubert, E. Riedle, A. Kiermeier, H. Kühlewind and E.W. Schlag, Ber. Bunserges. Phys. Chem., 92, 322 (1988).

65. C.E. Otis, J.L. Knee and P.M. Johnson, J. Phys. Chem., 87, 2232 (1983).

66. M. Sumitani, D. O'Connor, Y. Takagi, N. Kakashima, K. Kamogawa, Y. Udagawa and K. Yoshihara, Chem. Phys. Lett., 97, 508 (1983).

67. M. Sumitani, D.V. O'Connor, Y. Takagi, and K. Yoshihara, Chem. Phys. Lett., 108, 11 (1984).

68. D.V. O'Connor, M. Sumitani, Y. Takagi, N. Nakashima, K. Kamogawa, Y. Udagawa and K. Yoshihara, Chem. Phys., 93, 373 (1985).

69. M. Sumitani, D.V. O'Connor, Y. Takagi, N. Nakashima, K. Kamogawa, Y. Udagawa, and K. Yoshihara, Chem. Phys., 93, 359 (1985).

70. Y. Achilba, A. Hiraya and K. Kimura, J. Chem. Phys., 80, 6047 (1984).

71. T.A. Stephenson and S.A. Rice, J. Chem. Phys., 81, 1073 (1984).

72. T. Ichimura, H. Shinohara and N. Nishi, Chem. Phys. Letters, 146, 83 (1988).

73. M.G. Prais, D.F. Heller and K.F. Freed, Chem. Phys., 6, 331 (1974).

74. M. Kanamaru, Chemistry Lett., 503 (1978).

75. H. Hornburger and J. Brand, Chem. Phys. Lett. 88, 153 (1982).

76. S. Kato, J. Chem. Phys., 88, 3045 (1988).

77. W.M. McClain, J. Chem. Phys., 55, 2789 (1971).

78. P. Offenhartz, *Atomic and Molecular Orbital Theory*, (McGraw-Hill, New York) 340 (1970).

79. R. Destro, T.J. Kistenmacher, R.E. Marsh, Acta Cryst., B30, 79 (1974).

80. P.R. Callis, Chem. Phys. Lett., 107, 125 (1984).

81. R.D. Jones, Ph.D. Thesis, Montana State University (1987).

977-872